Лаборатория спутниковой океанографии

РГГМУ

Введение в спутниковую радиолокацию:

Радиолокаторы с синтезированной апертурой (РСА)

Introduction to satellite radars:

Synthetic Aperture Radars (SAR)

проф. Бертран Шапрон Prof. Bertrand Chapron

Outline

1. Intro to SAR basic principles
2. Range resolution
3. Phase history of a point target
4. Azimuth (along-track) resolution
5. Unfocused SAR
6. Focused SAR
7. Ocean applications

Envisat
ASAR

2002-2012

SAR = Synthetic Aperture Radar

An active instrument that transmit/receive EM radiation, store data in amplitude and phase (real and imaginary part)

- **Works in the presence of clouds, day and night**
- **Operates at microwave (or radar) frequencies**
- **Fine resolution is independent of the platform height, so images with the same geometric resolution (order of 10 m) can be obtained from satellites as from airplanes**

SAR principles:

- SAR is carried out on satellite with usually near-polar orbit, at an altitude ~600-800 km
- Antenna size is ~ 10 by 1 m
- Incidence angle between 15° and 60°

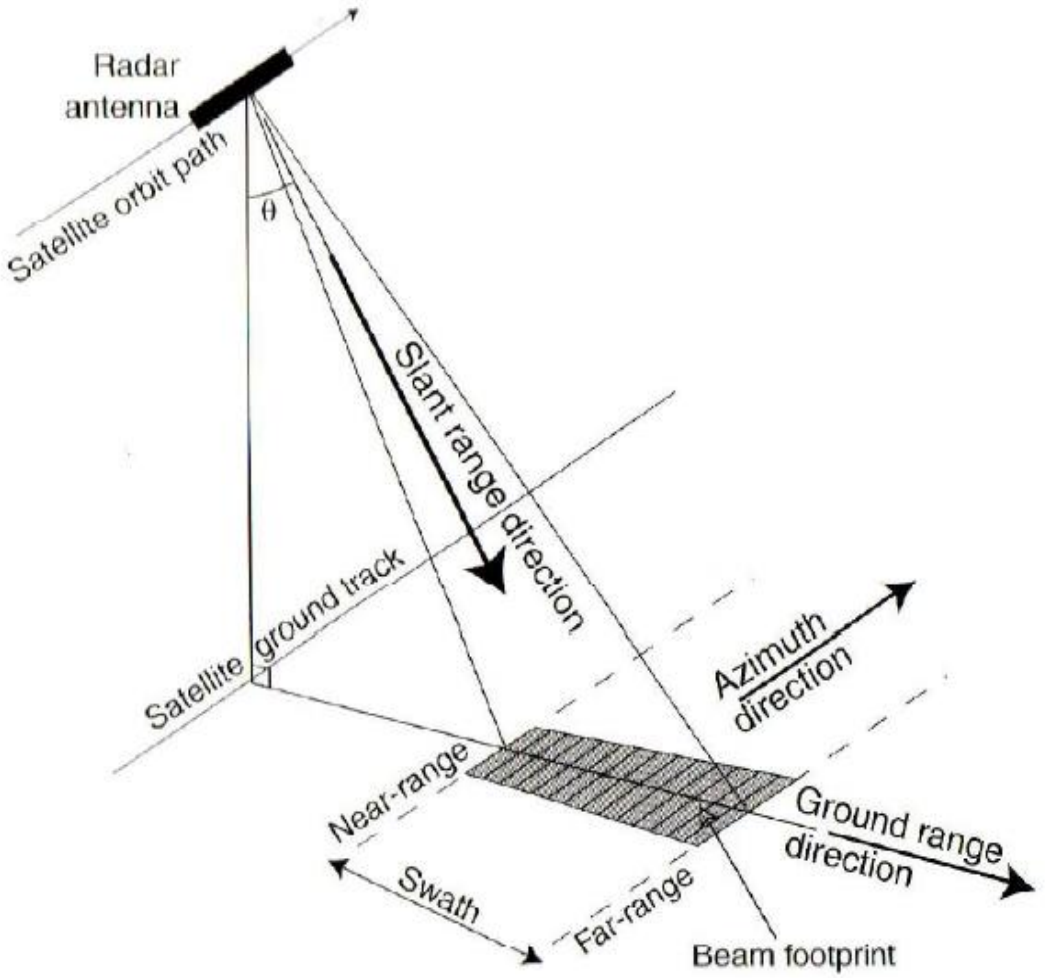

Figure 10.1. The general arrangement of a satellite SAR.

ANGLES AND RANGES

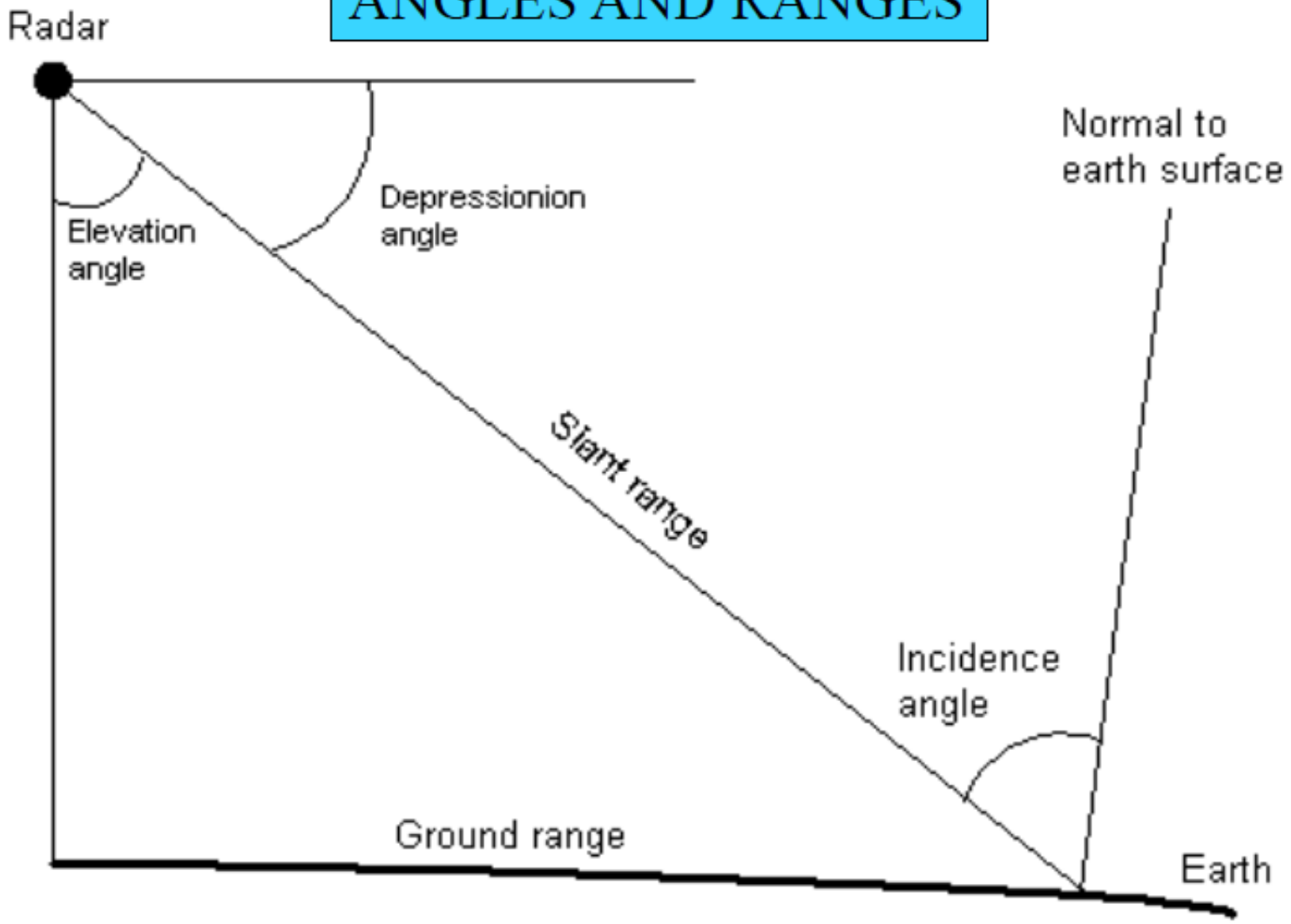

SAR imaging geometry

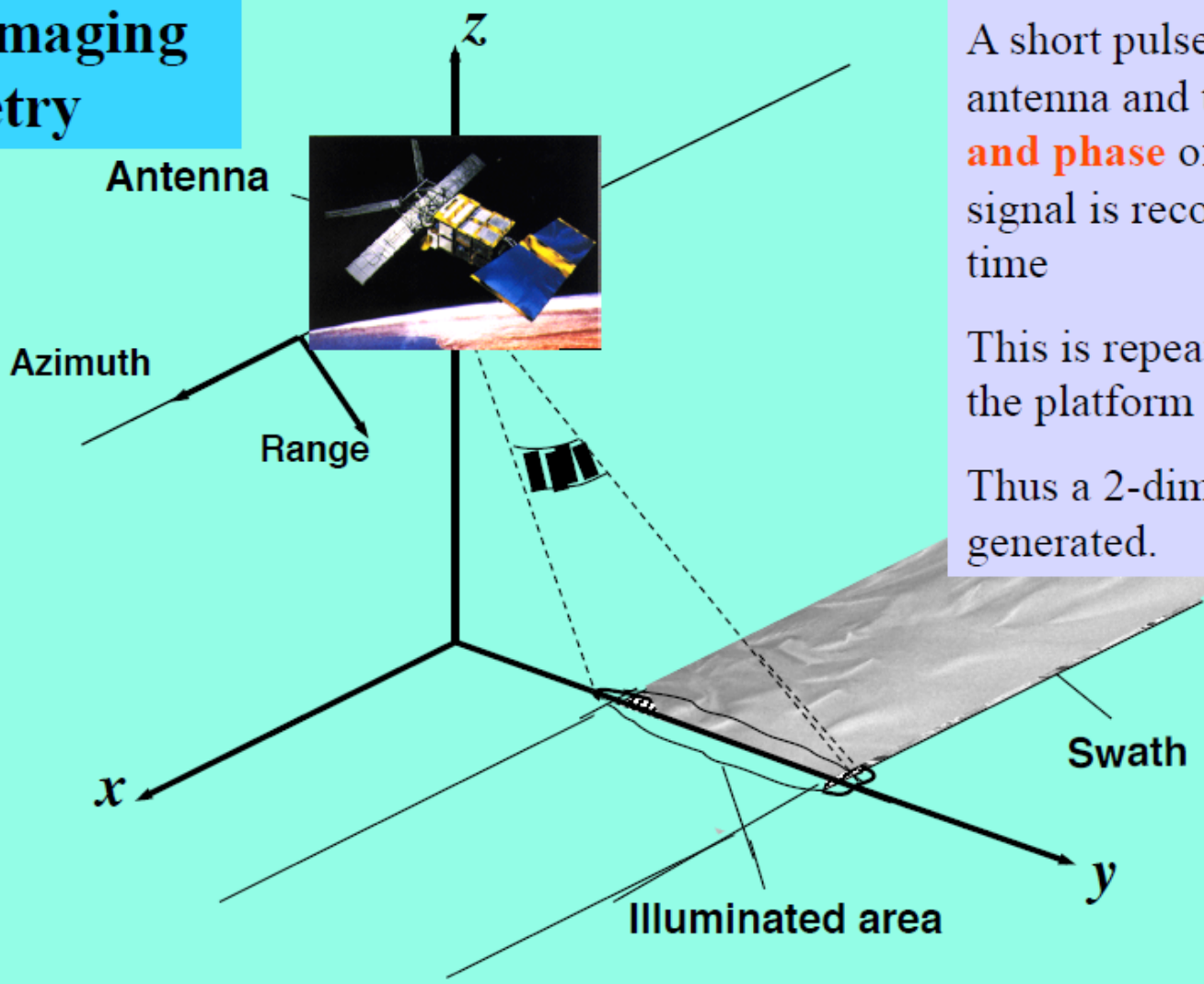

A short pulse is emitted by the antenna and then the **amplitude and phase** of the backscattered signal is recorded as a function of time

This is repeated over again while the platform is moving

Thus a 2-dimensional image is generated.

SAR principles

Short (microsecond) high energy pulses are emitted and the returning echoes recorded, providing information on:

- magnitude (or attenuation)
- phase
- time interval between pulse emission and return from the object
- polarization
- Doppler frequency

The same antenna is often used for transmission and reception.

SAR concept:

- SAR receives and records the echoes **coherently** – this needs a detector with a very high sampling rate

- Coherent recording of the echoes enables the **phase history** of individual scattering elements to be tracked

- Analysis of this coherent record from many echoes delivers **very fine resolution in azimuth and range** directions

$$\lambda = c * T = c * 1/f$$

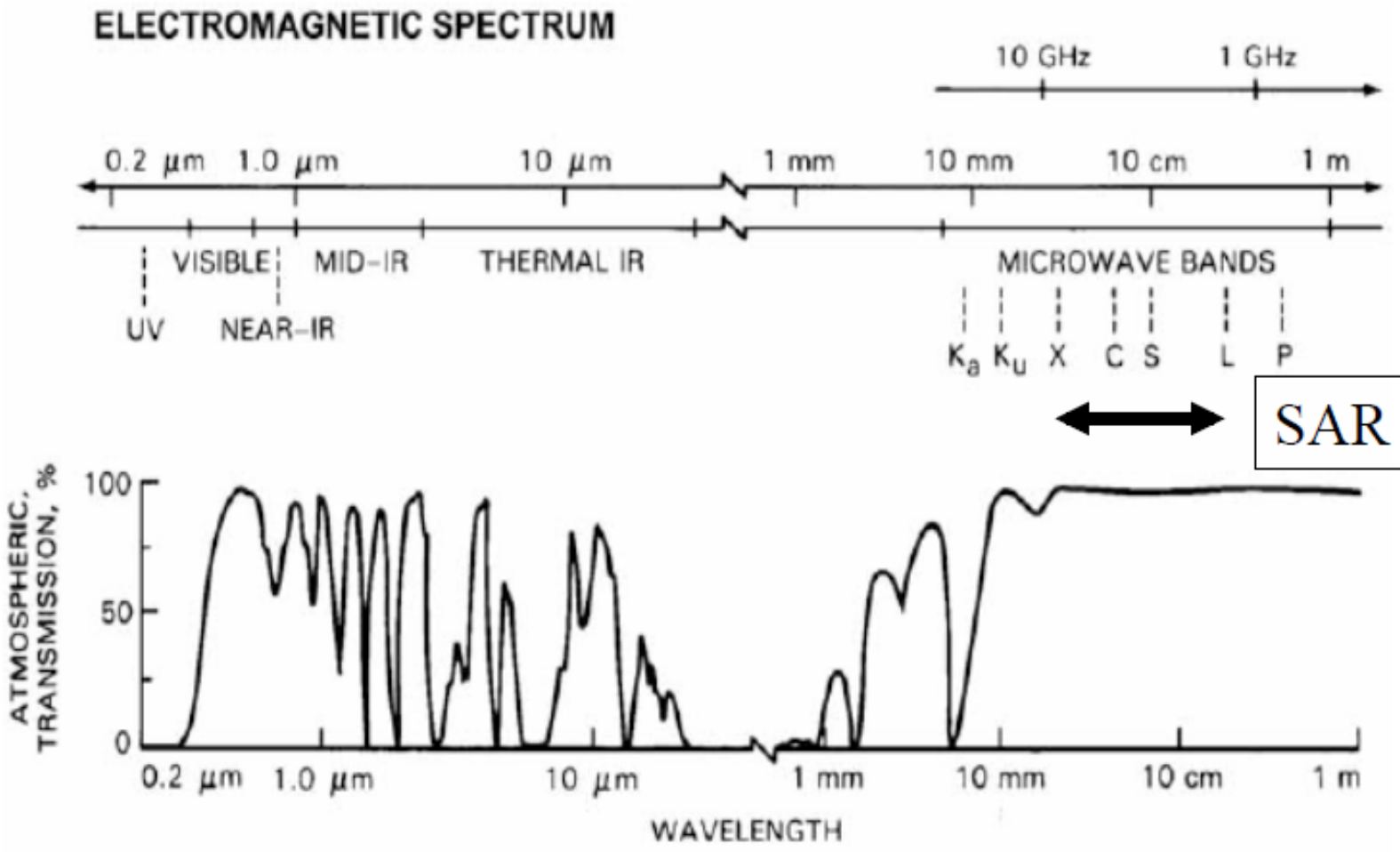

Azimuth resolution
SLAR systems

- The spatial resolution in the along-track direction (i.e. the azimuth) is determined by the angular width (or aperture) of the azimuth beam pattern (β)

ENVISAT case

λ_{radar} = 5.6 cm

L =10 m

R = 850 km

$\Rightarrow \delta_{az}$= 4.25km

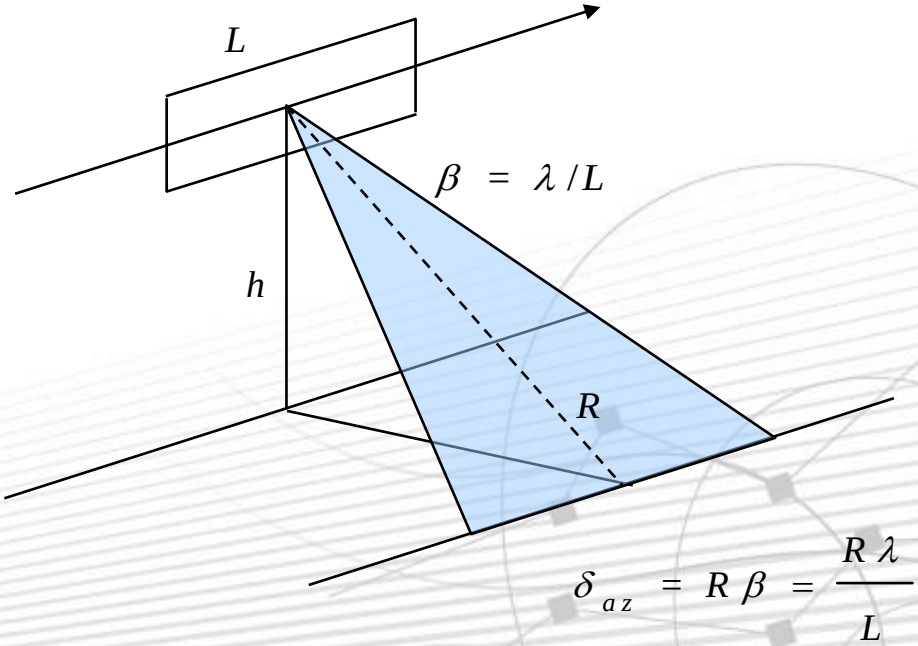

Azimuth resolution

Improving azimuth resolution: from SLAR to SAR

- Azimuth resolution is determined by the angular width of the azimuth beam pattern
  - resolution increases with range
  - smaller resolution means larger antennas ($\beta = \lambda/L$)
  - antennas became too large to realistically mount on an airplane

- This can be solved **by using a small antenna to "synthesize" what a larger antenna would have collected**, thus generating a synthetic antenna or aperture

Azimuth resolution
Synthetic Aperture Radar

- An artificial larger antenna is synthesized using displacement of the antenna along the track
- Finer azimuth resolution is achieved keeping track of the history of the Doppler frequency caused by the relative displacement of the target w.r.t. to the antenna.
- Best achievable resolution

$$\delta_{az} = \frac{L}{2}$$

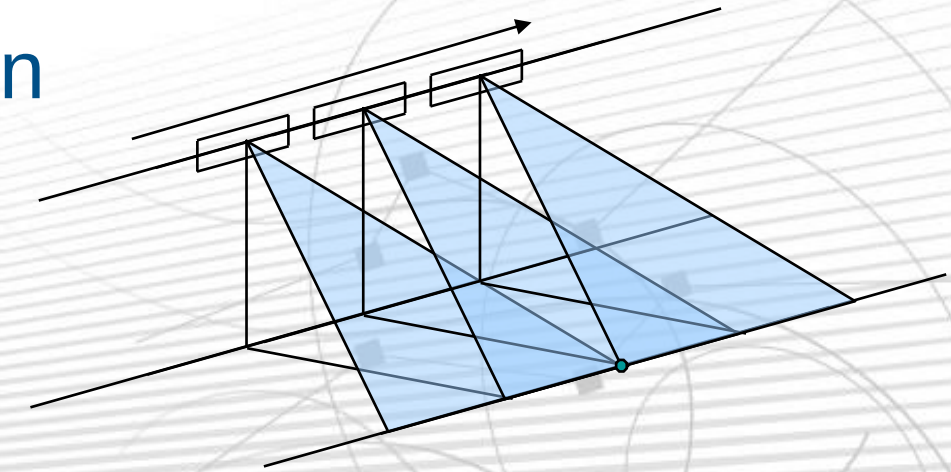

Range resolution

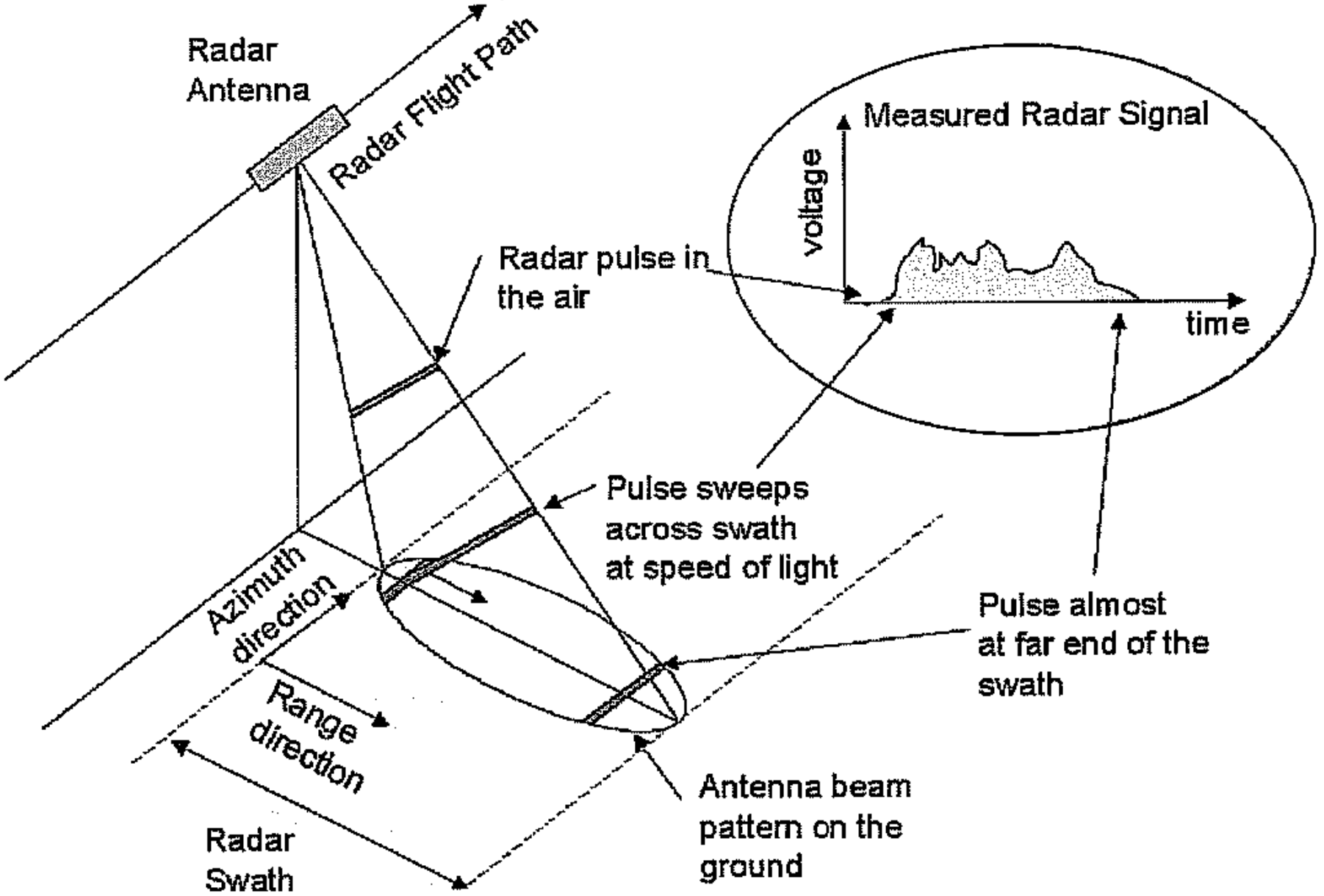

Figure 6-15. Imaging radars typically use antennas that have elongated gain patterns that are pointed to the side of the radar flight track. The pulse sweeps across the antenna beam spot, creating an echo as shown in this figure.

Phase history of a point target

Sensor moves along x-axes (azimuth) and emits radar pulses to the ground

The distance between the sensor at position *x* and the target can be expressed as

$$r = \sqrt{x^2 + r_0^2}$$

where r_0 denotes the minimum distance between them at $x=0$.

As the extension of the radar footprint on the ground is much smaller than the target distance ($x << r_0$), the following approximation can be made:

$$r = r_0\sqrt{1 + \frac{x^2}{r_0^2}} \approx r_0 + \frac{x^2}{2r_0}$$

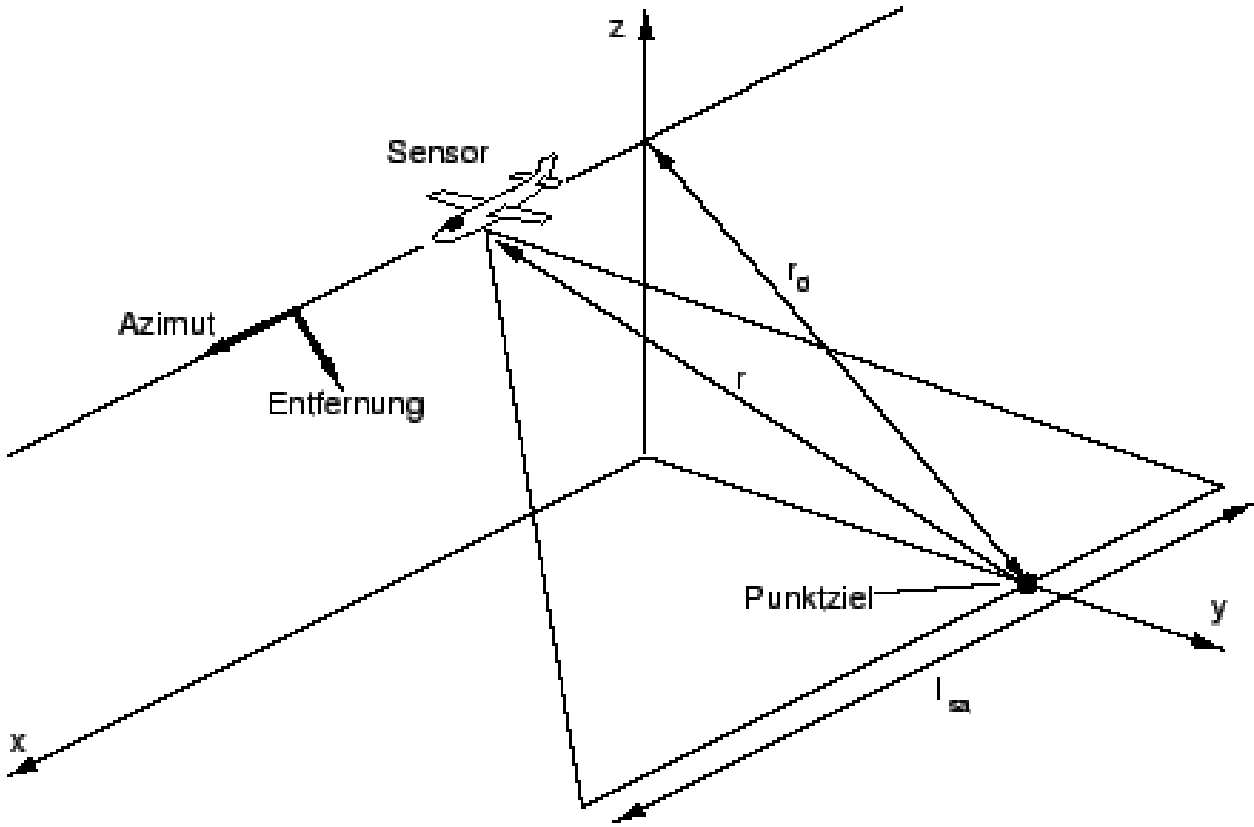

Along-track resolution

Consider a radar system flying at a constant speed along a straight and level trajectory as it views the terrain.

For a point on the ground the range to the radar and the radial velocity component can be determined as a function of time.

Radar position = $(0, v{\cdot}t, h)$, Target position = $(x_o, y_o, 0)$, Range to target, $R(t)$

$$R(t) = \sqrt{(0 - x_o)^2 + (v \cdot t - y_o)^2 + (h - 0)^2}$$

$$R(0) = \sqrt{x_o^2 + y_o^2 + h^2}$$

$$\frac{dR}{dt} = \dot{R}(t) = \frac{v(v \cdot t - y_o)}{\sqrt{x_o^2 + (v \cdot t - y_o)^2 + h^2}}$$

$$\dot{R}(0) = \frac{-y_o v}{\sqrt{x_o^2 + y_o^2 + h^2}}$$

$$f_D = -\frac{2}{\lambda}\dot{R}(0) = \frac{2 y_o v}{\lambda \sqrt{x_o^2 + y_o^2 + h^2}}$$

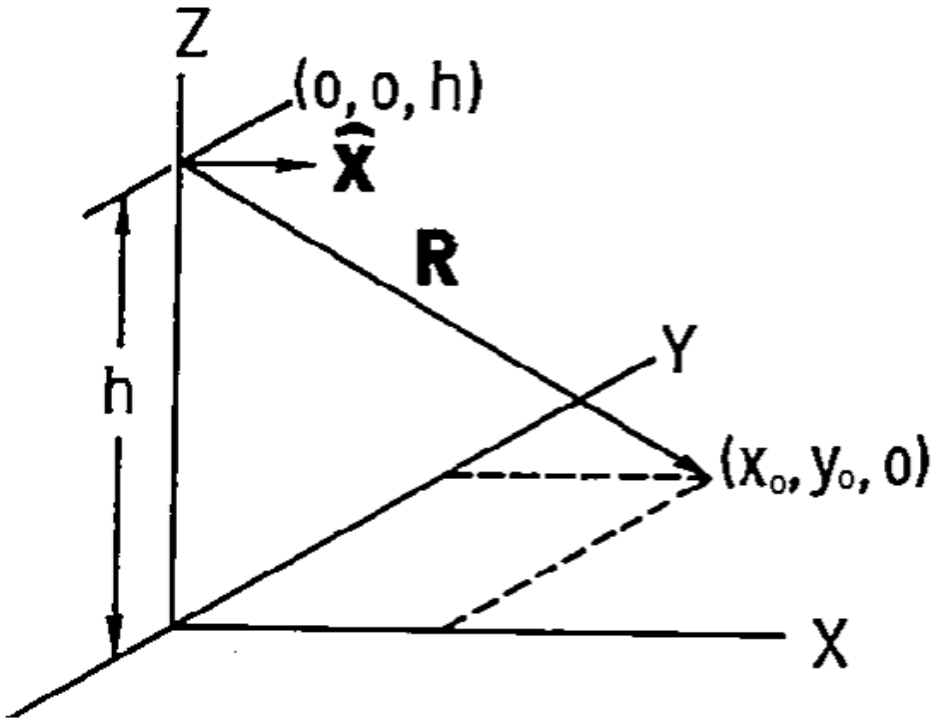

Phase history of a point target

The phases of the received echos, resulting from the two-way distance r, are:

$$\varphi(x) = 2\frac{2\pi}{\lambda}\left(r_0 + \frac{x^2}{2r_0}\right) = \frac{2\pi x^2}{\lambda r_0} + \text{const.} \qquad (10)$$

Assuming a constant sensor velocity v and the abbreviation $k = 2\pi v^2/\lambda r_0$, a quadratic phase behaviour in time is resulting, neglecting the constant phase term, which has no time dependency.

$$\varphi(t) = kt^2$$

The quadratic phase behaviour corresponds to a linear change in the received azimuth frequency $f(t)$, the so-called DOPPLER-effect.

$$f(t) = \frac{1}{2\pi}\frac{\partial\varphi(t)}{\partial t} = \frac{k}{\pi}t \qquad (12)$$

Phase history of a point target

The maximal illumination time of a point target is defined by the extension of the antenna footprint in azimuth. This length, equal to the length of the synthetic aperture, is determined by:

$$t_{max} = \frac{l_{sa}}{v} = \frac{\theta_{ra} r_0}{v}$$

The bandwidth of the signal in azimuth B_a is, therefore,

$$B_a = f(-t_{max}/2) - f(+t_{max}/2) = \frac{2v\theta_{ra}}{\lambda}$$

This bandwidth in azimuth sets also the lower limit of the pulse repetion frequency (PRF) of the radar, with which the radar pulses are emmitted to the ground. After eliminating the carrier frequency (demodulation in the receiver hardware), frequencies between $-B_a/2$ and $+B_a/2$ are present in the complex signal.

Unfocused SAR

Processing SAR phase data to achieve a fine-resolution image requires elaborate signal processing.

In some cases trading off resolution for processing complexity is acceptable.

In these cases a simplified ***unfocused* SAR** processing is used wherein only a portion of the azimuth phase history is used resulting in a coarser azimuth resolution.

In unfocused SAR processing consecutive azimuth samples are added together (in the slow-time domain).

Since addition is a simple operation for digital signal processors, the image formation processing is much easier (less time consuming) than fully-focused SAR processing.

Unfocused SAR

Summing consecutive samples, also known as a *coherent integration* or *boxcar filtering*, is useful so long as the signal's phase is relatively constant over the integration interval.

Example

For a 20-sample interval the central portion of the chirp waveform (zero Doppler) is relatively constant.
For the outer portions of the chirp the phase varies significantly and integrating produces a reduced output.

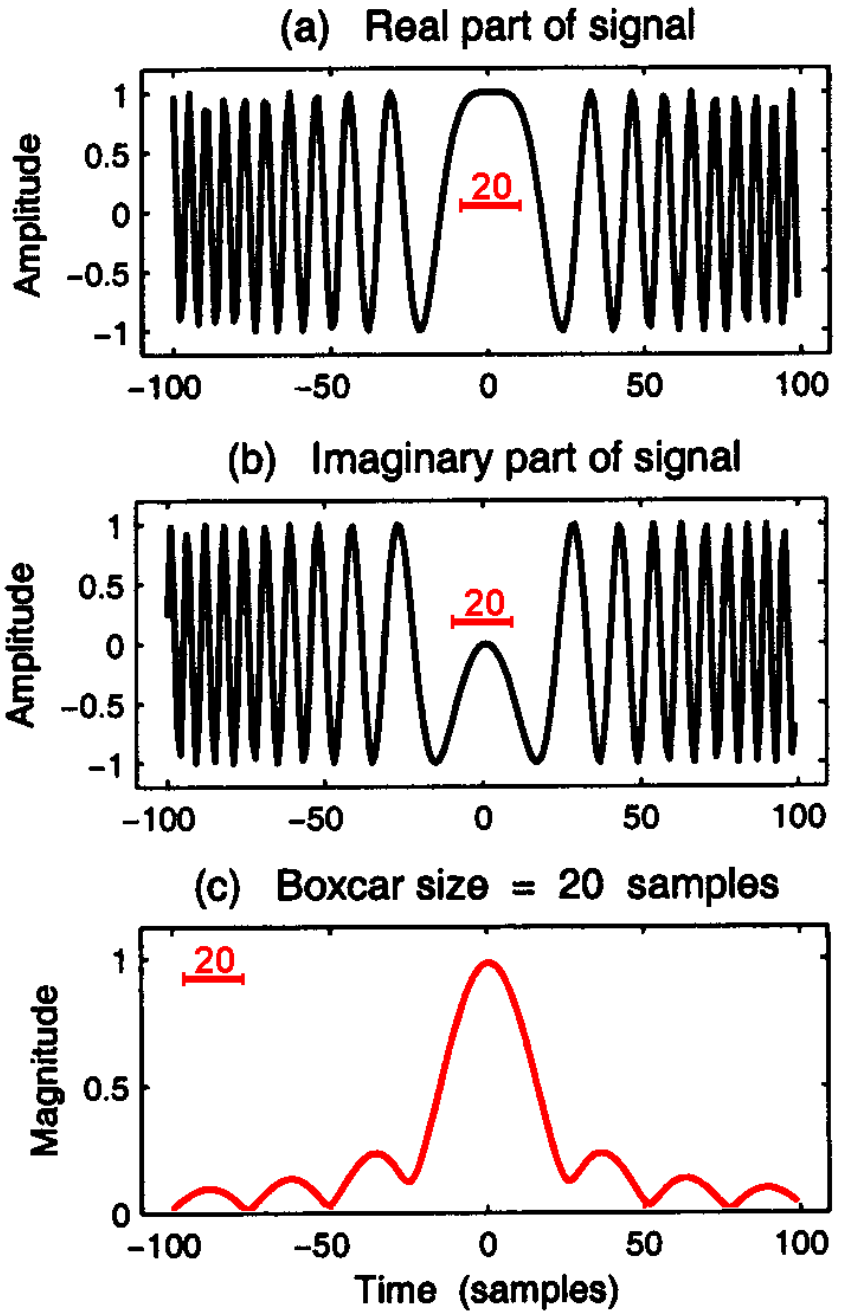

Figure 5.21: Boxcar filtering applied to linear FM signal.

Unfocused SAR

Example (cont.)

Over a 38-sample interval phase variations within the central portion of the chirp waveform results in a reduced output (0.8 peak vs. 1).

The magnitude of the first sidelobe is also larger (0.4 vs. 0.3).

The width of the main lobe is narrower.

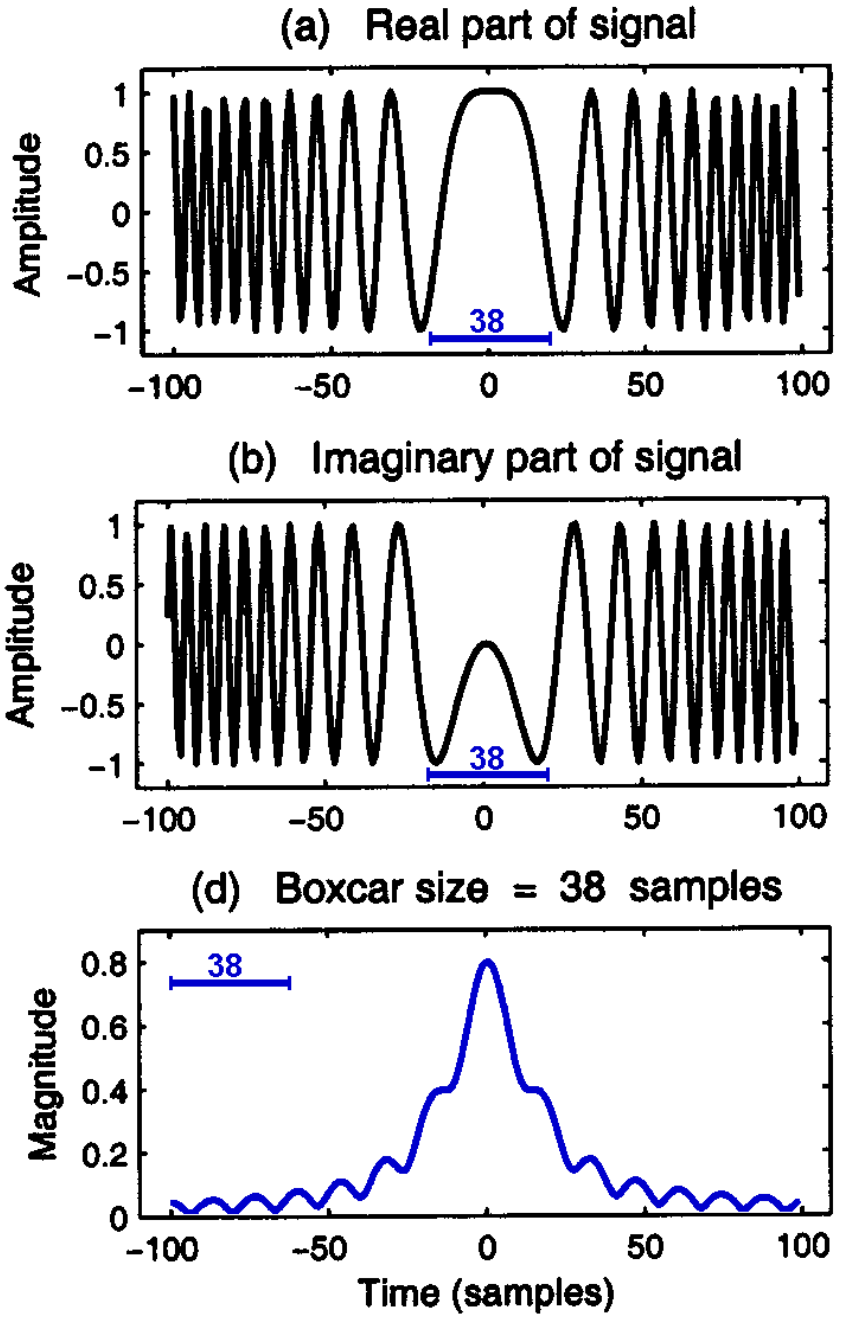

Figure 5.21: Boxcar filtering applied to linear FM signal.

Unfocused SAR

The resolution improves with increased integration length up to a point when oscillations in the signal are included in the integral.

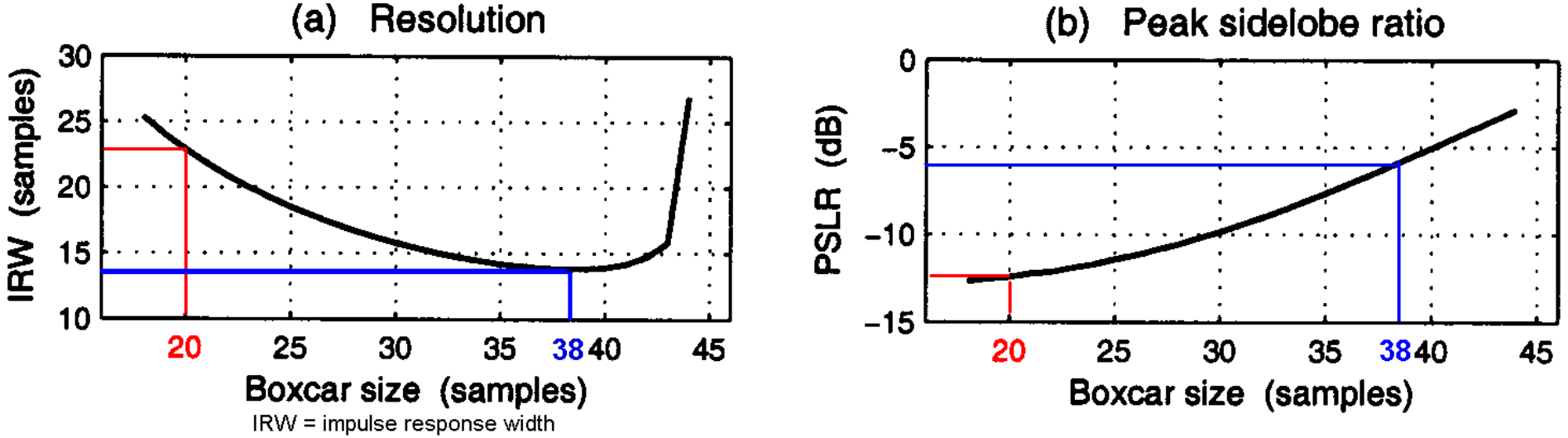

Figure 5.22: Resolution and sidelobe ratio for unfocused SAR processing.

The maximum synthetic aperture length for unfocused SAR is L_u which corresponds to a maximum phase shift across the aperture of 45º.

$$L_u = \sqrt{R\ \lambda / 2}\ , \quad (m)$$

The azimuth resolution for $L = L_u$ is

$$\Delta y = \sqrt{R\ \lambda / 2}\ , \quad (m)$$

Notice the range- and frequency-dependencies of Δy.

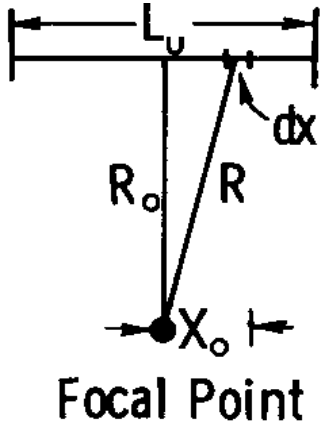

Focused SAR

To realize the full potential of SAR and achieve fine along-track (azimuth) resolution requires matched filtering of the azimuth chirp signal.

Stretch chirp processing, correlation processing, tracking Doppler filters, as well as other techniques can be used in a matched filter process.

However the range processing is not entirely separable from the azimuth processing as an intricate interaction between range and azimuth domains exists which must also be dealt with to achieve the desired image quality.

Focused SAR

In SAR systems a very long antenna aperture is synthesized resulting in fine along-track resolution.

For a synthesized-aperture length, L, the along-track resolution, Δy, is

$$\Delta y = \lambda R / (2L)$$

L is determined by the system configuration.

For a fully focused stripmap system, $L_m = \beta_{az} \cdot R \ (m)$, where

β_{az} is the azimuthal or along-track beamwidth of the real antenna ($\beta_{az} \cong \lambda/\ell$)

R is the range to the target

For $L = L_m$, $\Delta y = \ell/2$ (independent of range and wavelength)

Processing in azimuth

The echo of a single point target is contained in many received radar pulses and appears defocused.

The aim of SAR processing, or **compression**, is to focus all received energy of a target on one point at t=0.

To achieve this, phase history is used. The received signal in the azimuth direction can be rewritten as

$$S_a(t) = A_0 \exp(i\varphi(t)) = A_0 \exp(ikt^2)$$

Where A_0 denotes the backscatter amplitude of a point target (complex).

The idea of azimuth compression is to adjust all phase values to the same value followed by coherent summation.

To achieve this, a correlation of $S_a(t)$ with a reference function $R(t) = \exp(-ikt^2)$ is performed.

The reference function has exactly opposite phase.

The result of the correlation is then

$$V(t) = \int_{-\infty}^{\infty} S_a(\xi) R(t+\xi) d\xi \tag{18}$$

$$= \int_{-\infty}^{\infty} A_0 \exp(ik\xi^2) \exp(-ik(t+\xi)^2) W(t+\xi) d\xi \tag{19}$$

$$= A_0 \exp(-ikt^2) \int_{-\infty}^{\infty} W(t+\xi) \exp(-2ik\xi t) d\xi \tag{20}$$

Or after applying FT:

$$\Longrightarrow \qquad V(t) = A_0 t_{max} \sqrt{2\pi} \exp(-ikt^2) \left[\frac{\sin(kt_{max}t)}{kt_{max}t} \right] \tag{25}$$

The result of this correlation is the image. The principal shape of the resulting impulse response corresponds thereby to the FOURIER-transform of the weigthing function.

In Fig. 3.2 this process is illustrated.

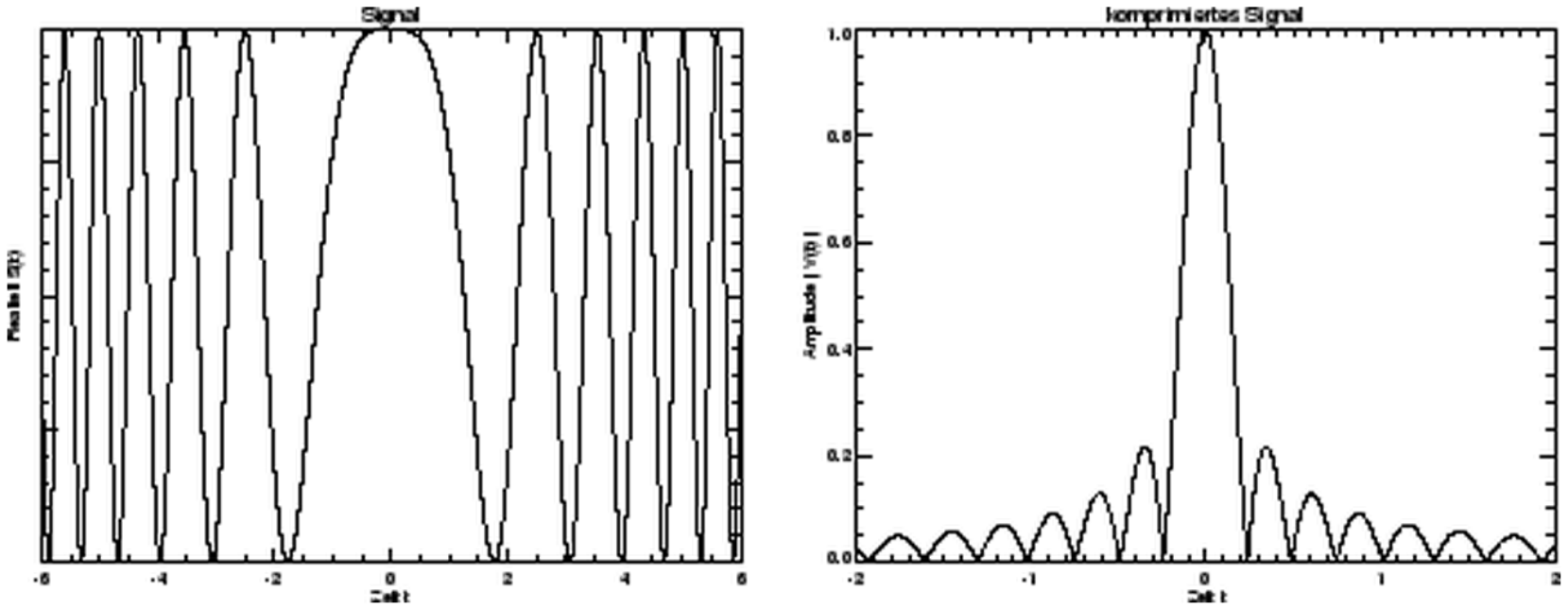

Figure 3.2: Signal compression. Real part of the complex signal of an ideal point target response (left) and amplitude of the compressed signal (right).

Defining the resolution as the half distance between the first minima of the main peak at $t = \pm\pi / kt_{max}$, a synthetic aperture consequently has an azimuthal resolution of:

$$\delta_{sa} = \frac{\pi v}{kt_{max}} = \frac{v}{B_a} = \frac{l_{ra}}{2} \tag{26}$$

Along-track resolution

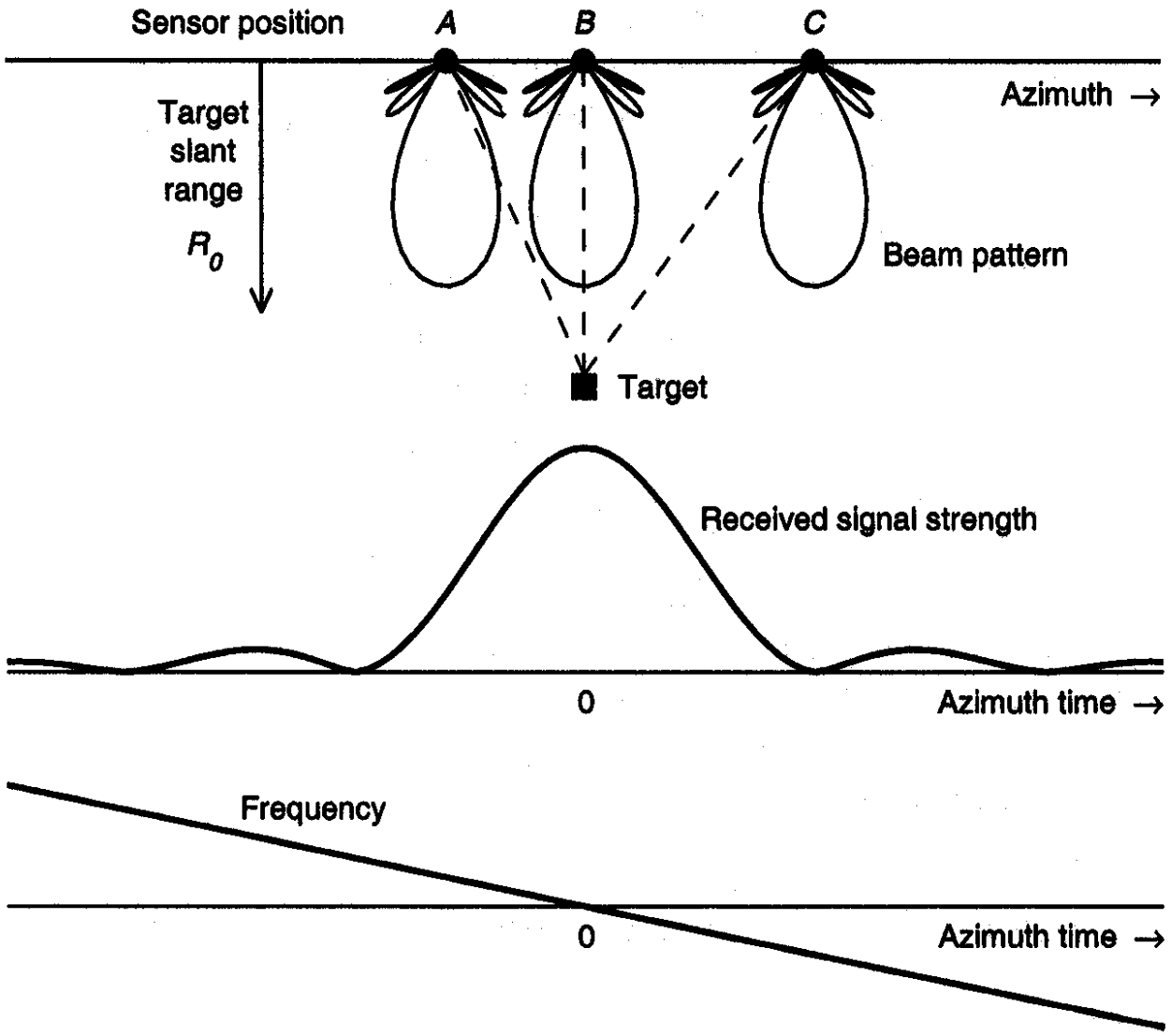

Figure 4.10: Azimuth beam pattern and its effect upon signal strength and Doppler frequency.

SAR processor

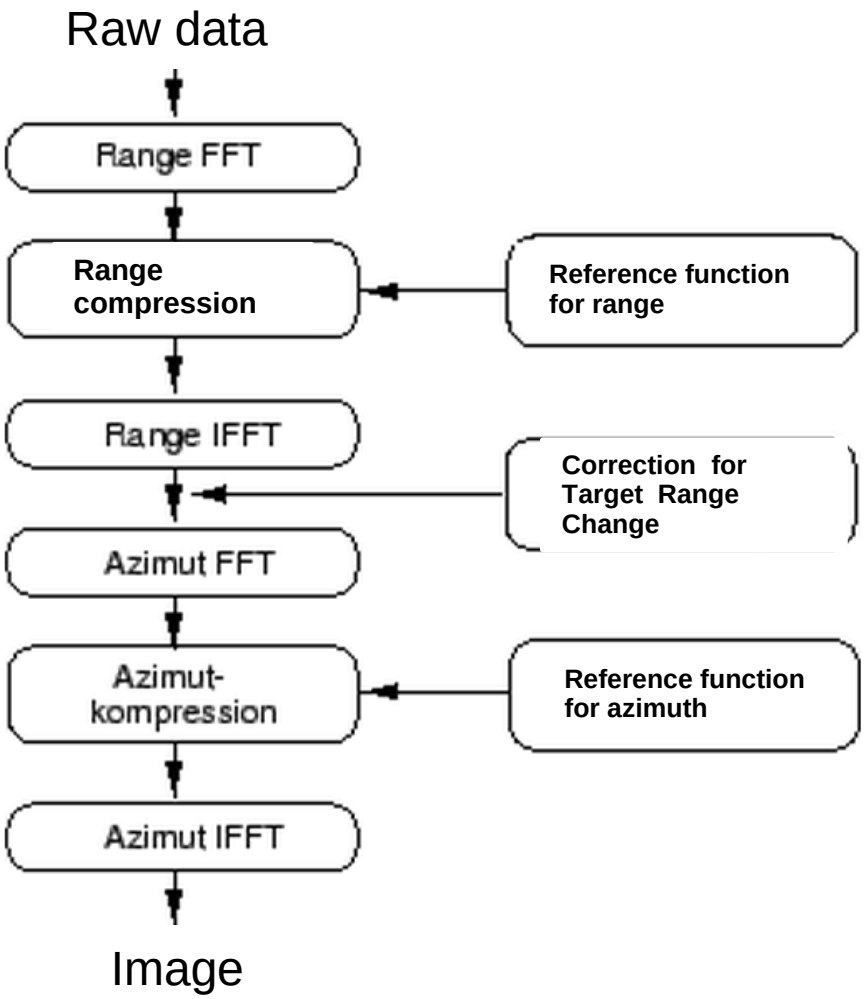

Figure 3.5: Block-diagram of a simple SAR processor

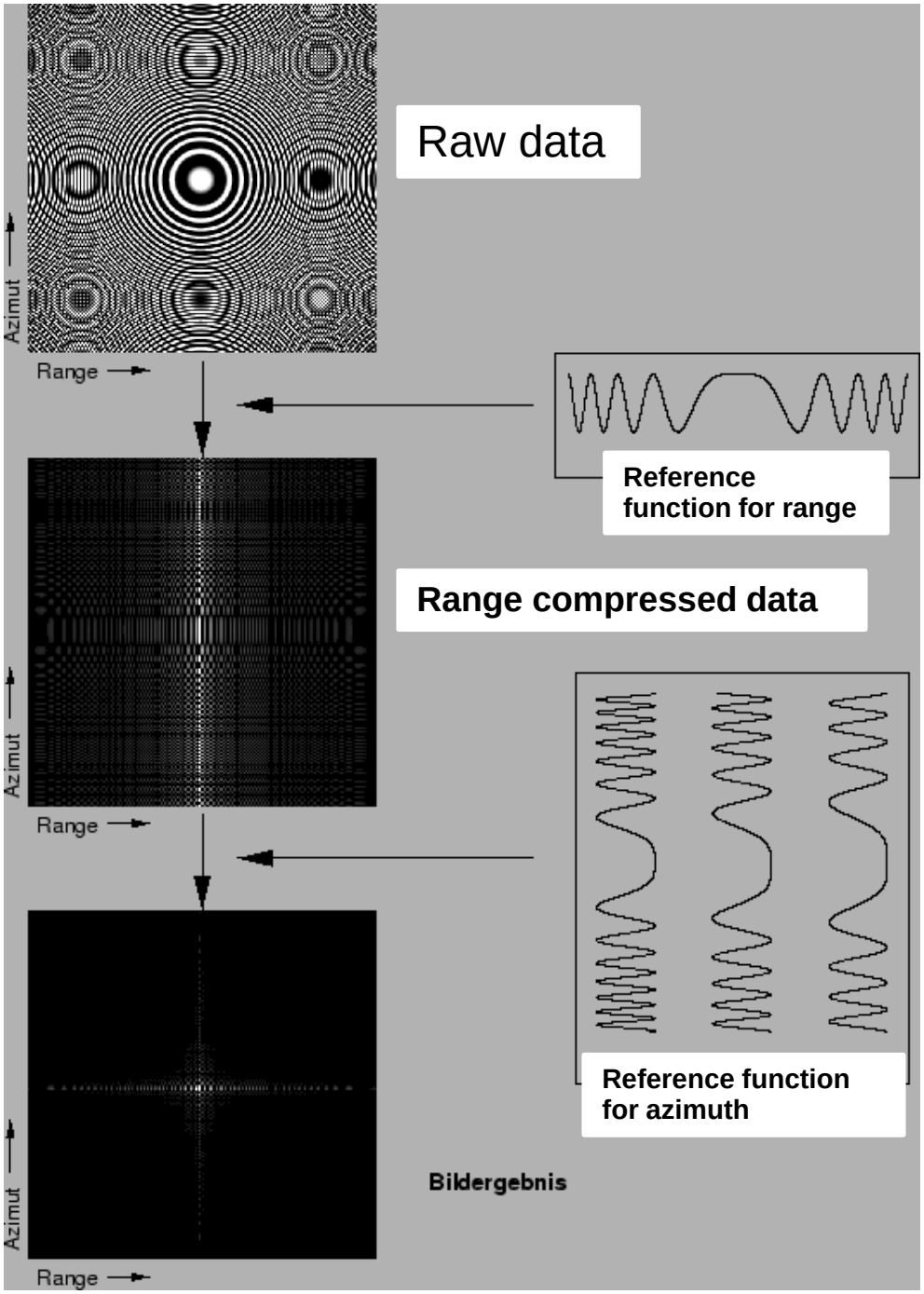

SAR processing example

Reading and visualizing the raw data

STAGES IN SAR IMAGE COMPRESSION

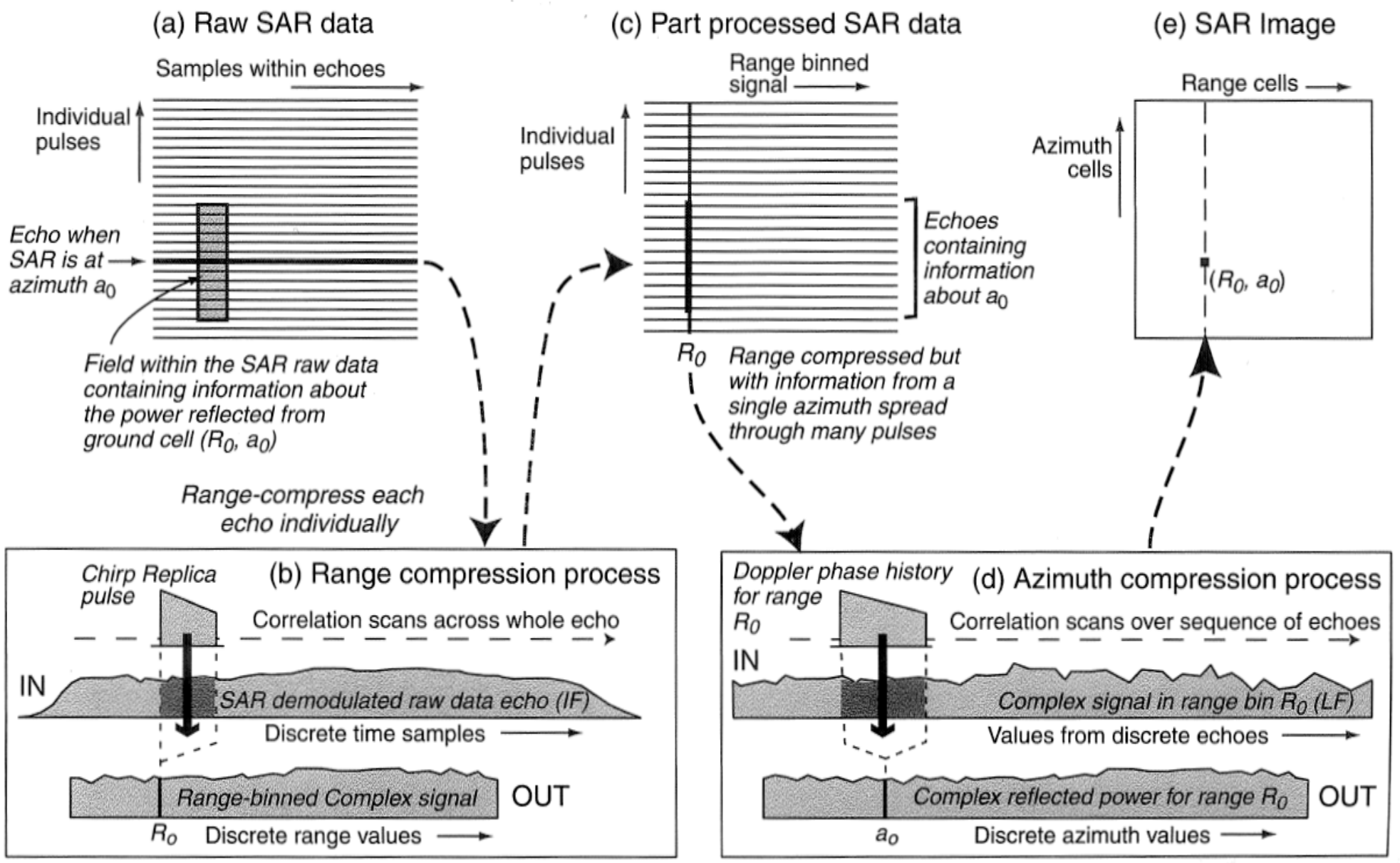

Ocean applications

New Ocean Waves Algorithm/Product

Level 1

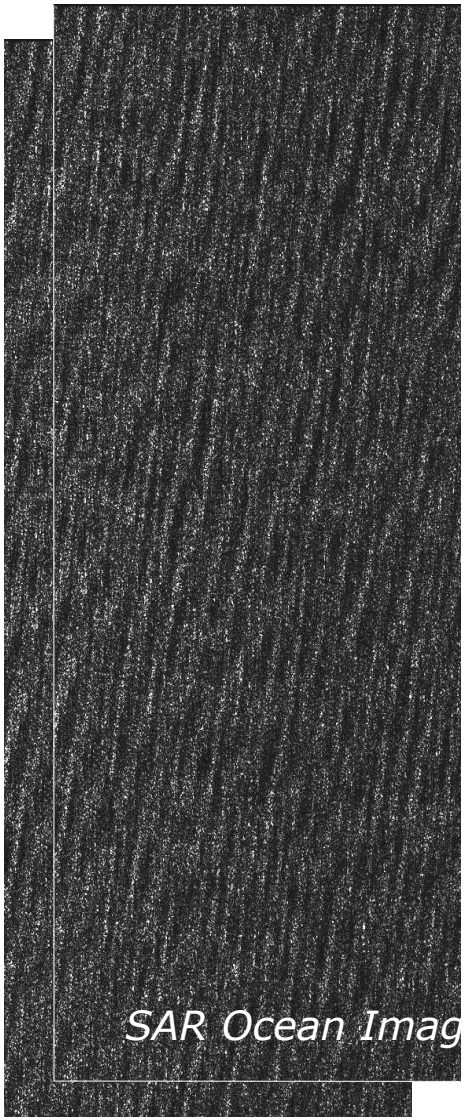

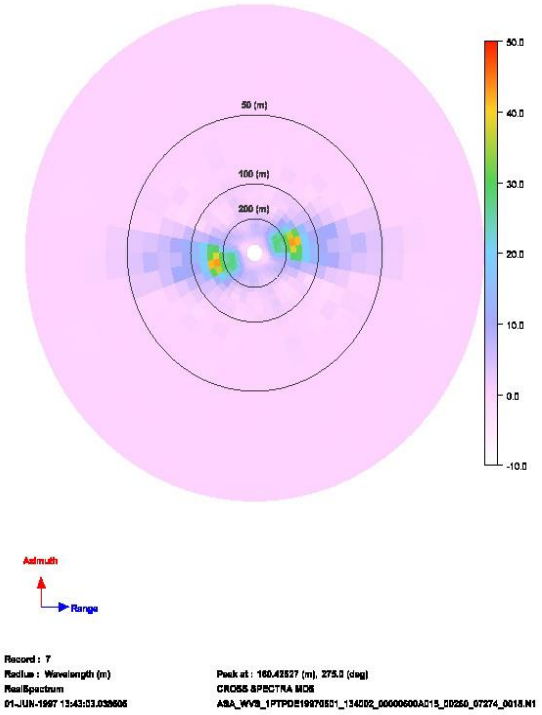

Real Part

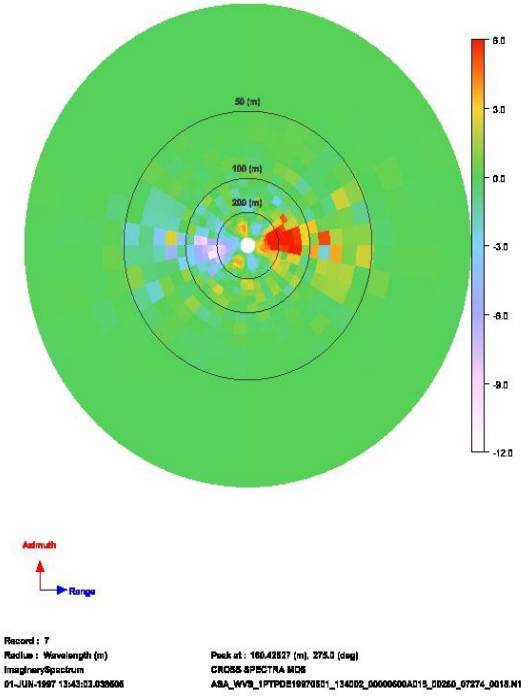

Imaginary Part

A decisive breakthrough : the cross-spectral analysis

- Based on ERS Image products, G. Engen and H. Johnsen (NORUT) proposed the use of Single Look Complex (SLC) imagettes using cross-spectra methodology (*Engen et al., 1995, TGARS*)

Improvements:

- Direct uncorrelated noise removal
- Hands-off resolved wave propagation ambiguity in most cases (85%)

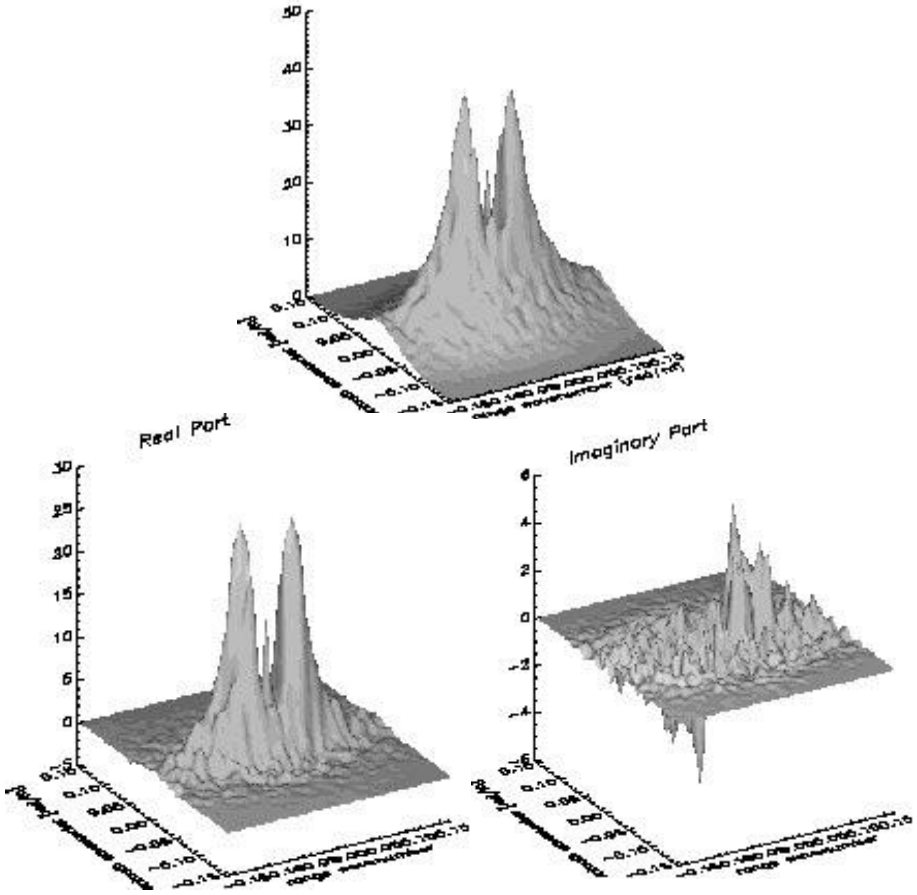

New algorithm philosophy

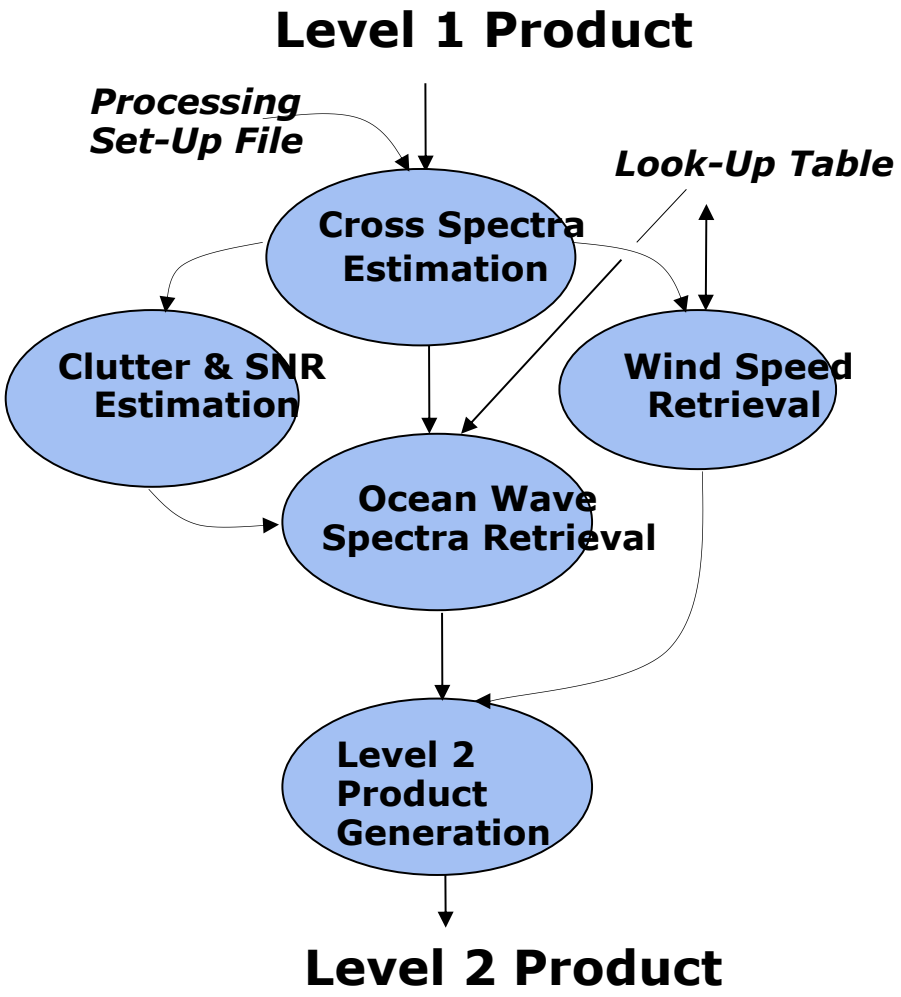

Inversion Model:

where

$$\chi^{nlin}(\underline{k};U_{10}); \quad from\ look-up\ table$$

$$T(\underline{k}) = \left\{ ik_y \frac{R}{V} \omega_k + 2k_{rad} k_x \nabla\sigma \right\} G(\theta)$$

$$G(\theta) \equiv \frac{k_x}{|\underline{k}|} \sin\theta + i\cos\theta$$

$$\nabla\sigma \equiv \frac{\Delta\sigma_{c\,\mathrm{mod}}}{\Delta\theta} \frac{1}{\sigma_{c\,\mathrm{mod}}} \frac{1}{2k_{rad}\cos\theta}$$

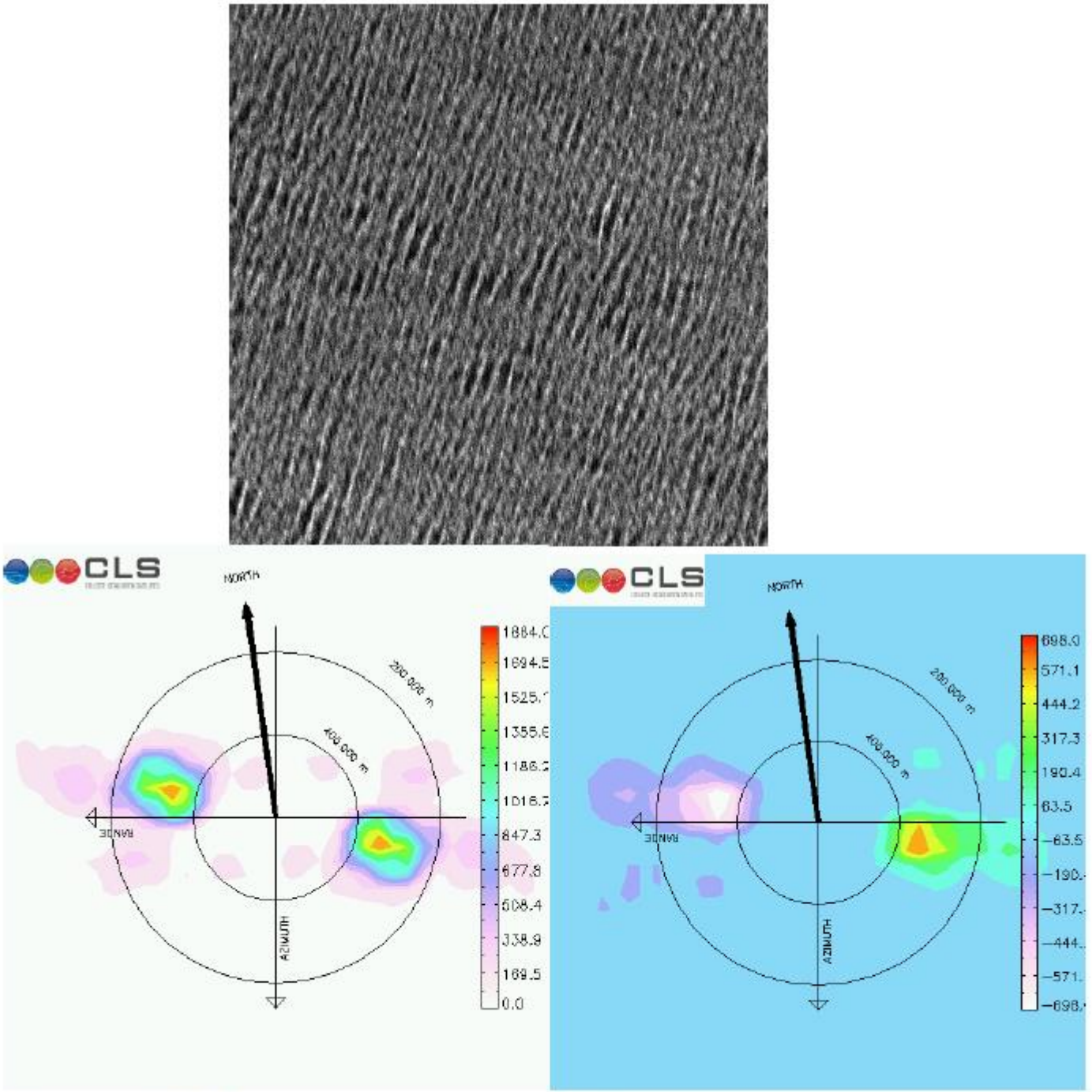

Figure 18 : HIMAGE cross-spectrum. Image intensity(top), real part of cross spectra (left), imaginary part of cross-spectra (right).

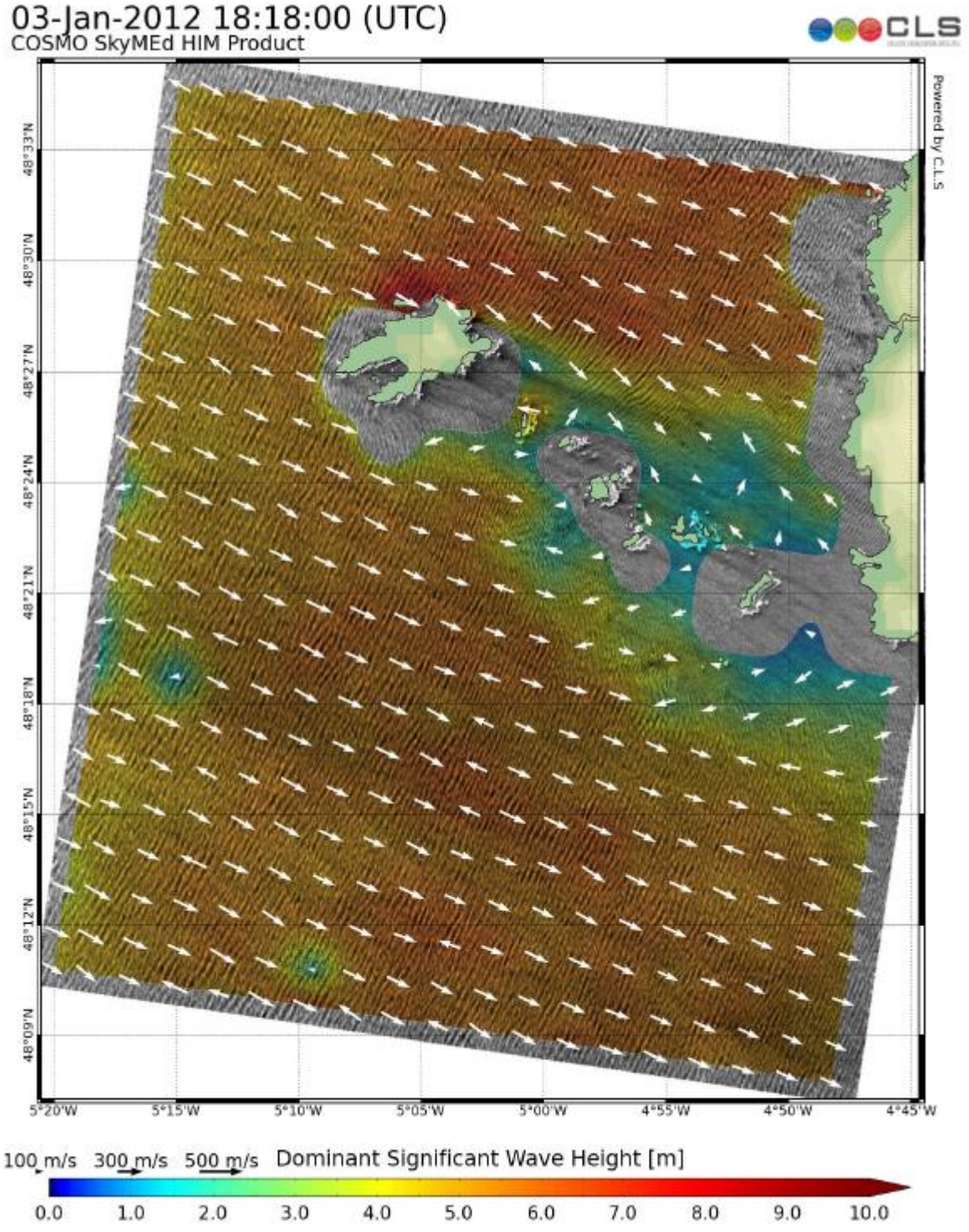
03-Jan-2012 18:18:00 (UTC)
COSMO SkyMEd HIM Product
CLS
Powered by C.L.S
48°33'N
48°30'N
48°27'N
48°24'N
48°21'N
48°18'N
48°15'N
48°12'N
48°09'N
5°20'W
5°15'W
5°10'W
5°05'W
5°00'W
4°55'W
4°50'W
4°45'W
100 m/s
300 m/s
500 m/s
Dominant Significant Wave Height [m]
0.0
1.0
2.0
3.0
4.0
5.0
6.0
7.0
8.0
9.0
10.0

ERS data as testbed for ENVISAT

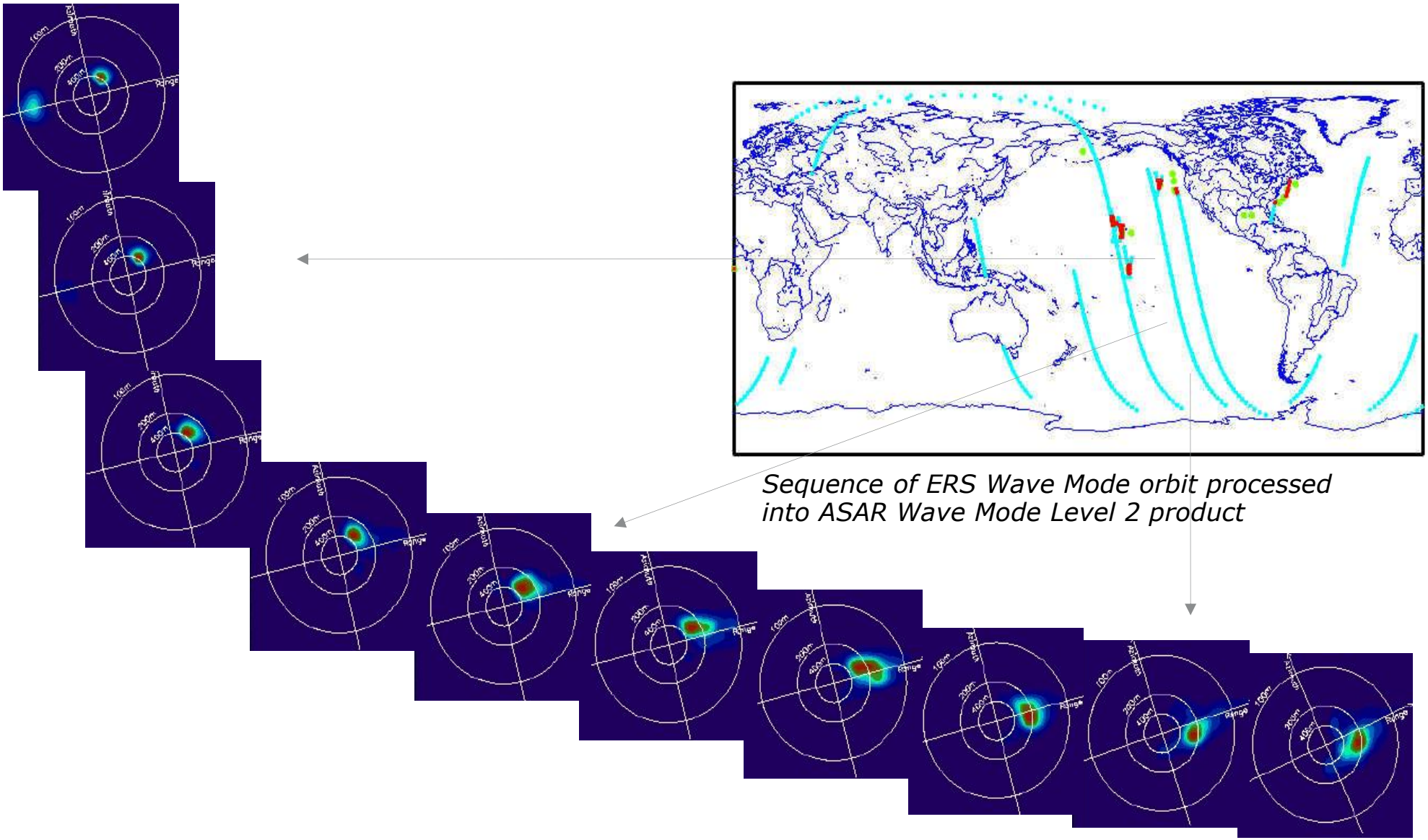

Sequence of ERS Wave Mode orbit processed into ASAR Wave Mode Level 2 product

Fireworks

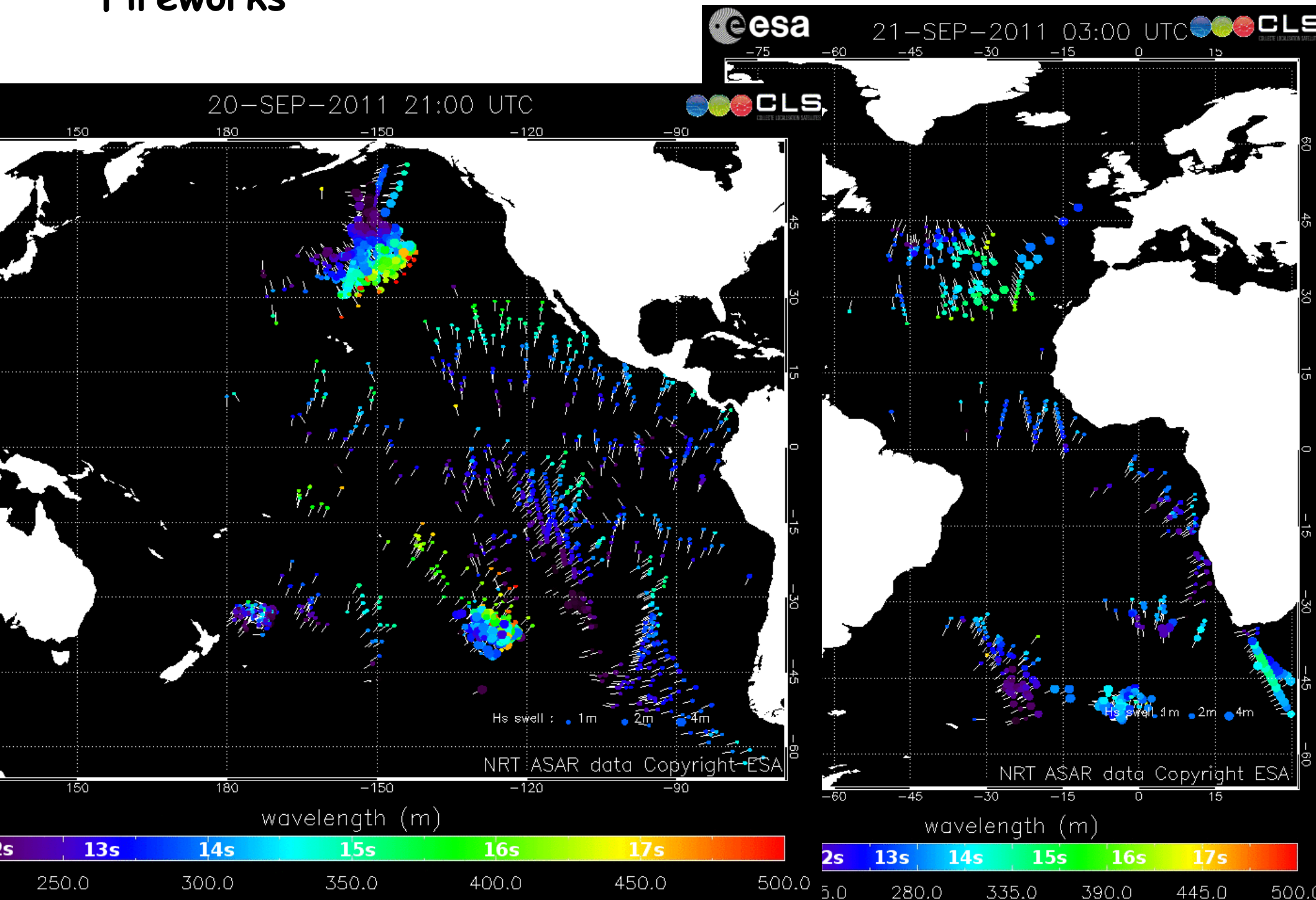
20-SEP-2011 21:00 UTC
CLS
Hs swell : 1m 2m 4m
NRT ASAR data Copyright ESA
wavelength (m)
13s 14s 15s 16s 17s
250.0 300.0 350.0 400.0 450.0 500.0
esa
21-SEP-2011 03:00 UTC
CLS
Hs swell : 1m 2m 4m
NRT ASAR data Copyright ESA
wavelength (m)
2s 13s 14s 15s 16s 17s
280.0 335.0 390.0 445.0

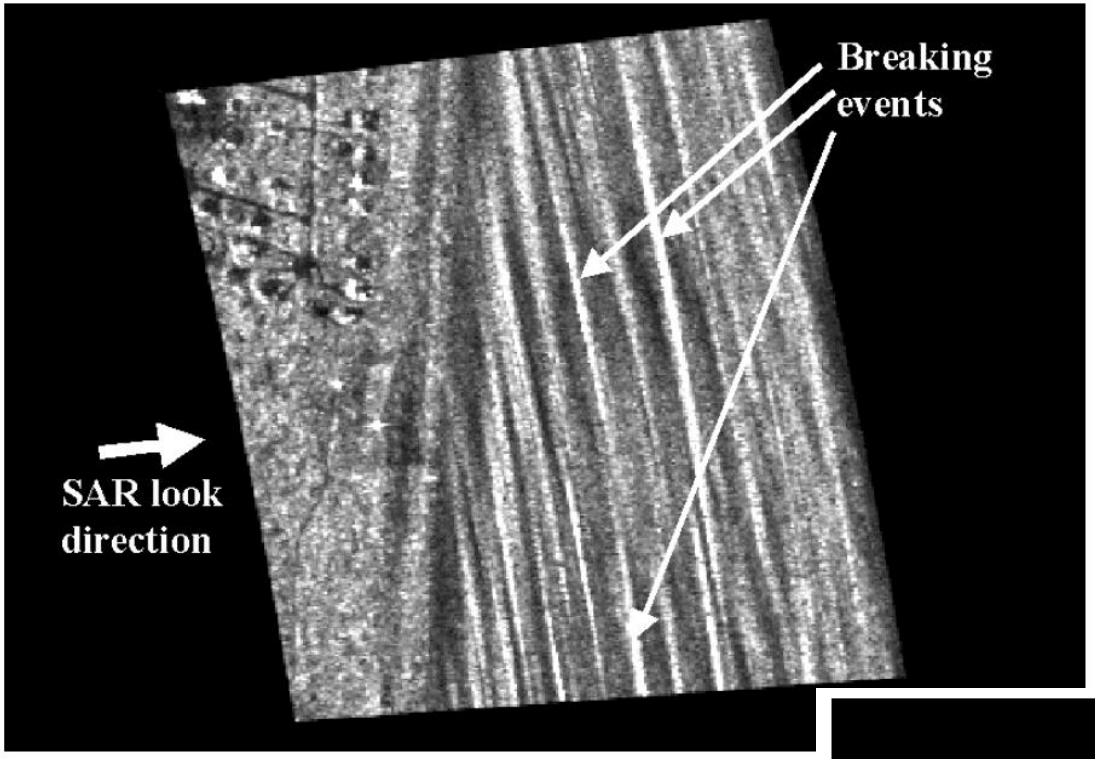
Breaking
events
SAR look
direction

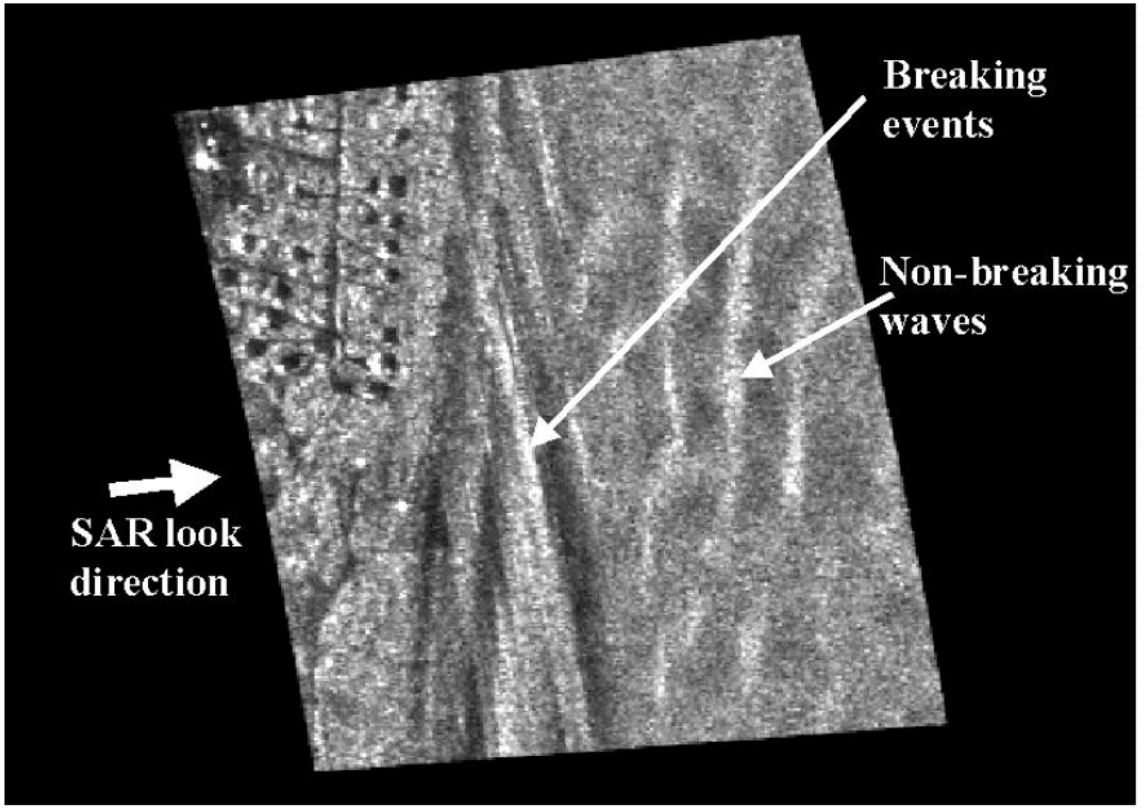
Breaking
events
Non-breaking
waves
SAR look
direction

- **Ocean currents retrieved from SAR Doppler shifts**

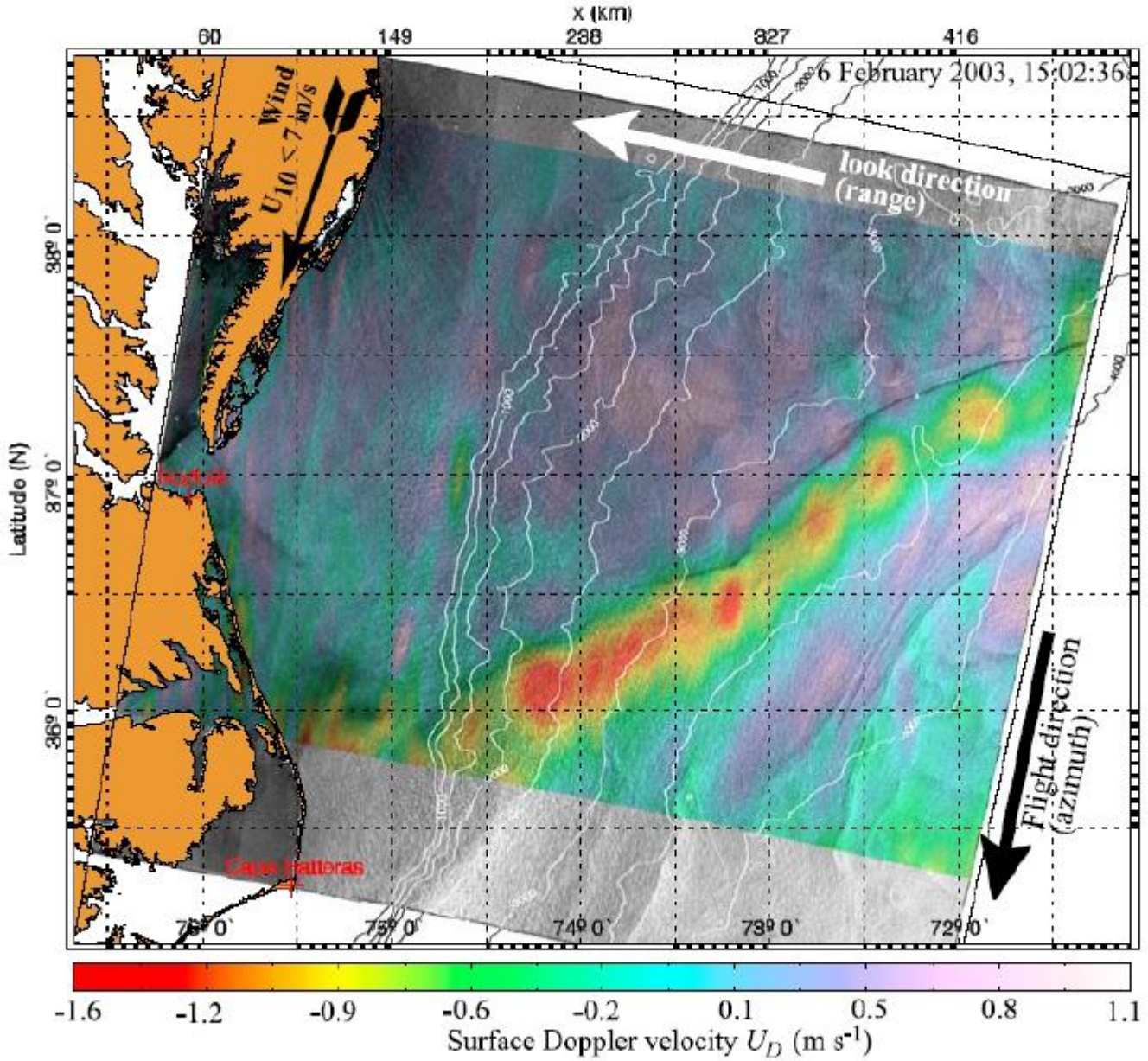

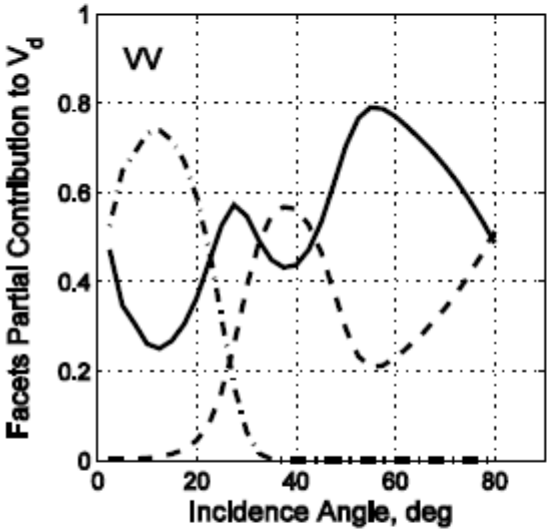

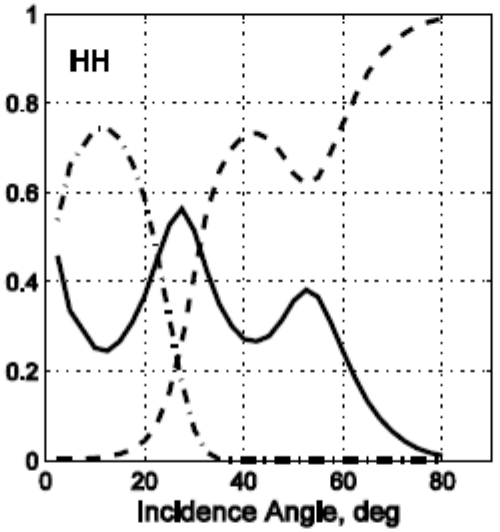

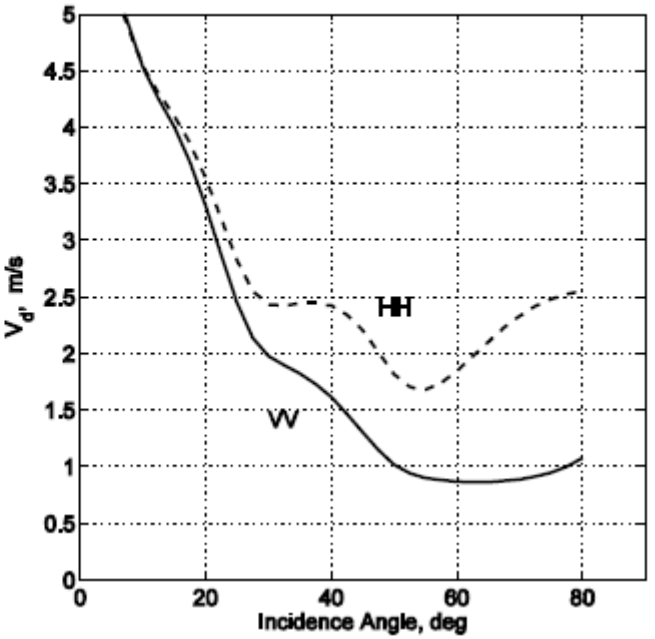

- C-band Doppler velocities for VV (solid line) and HH (dashed line) vs. incidence angle at 10 m/s wind speed

- Partial contribution of different type of facets to the total C-band Doppler velocity at wind speed 10m/s for VV (left) and HH (right) polarizations.
- Solid lines are for Bragg-facet,
- dash-dotted lines are for mirror points,
- dashed lines are for breakers.

• Doppler shift: Main equation

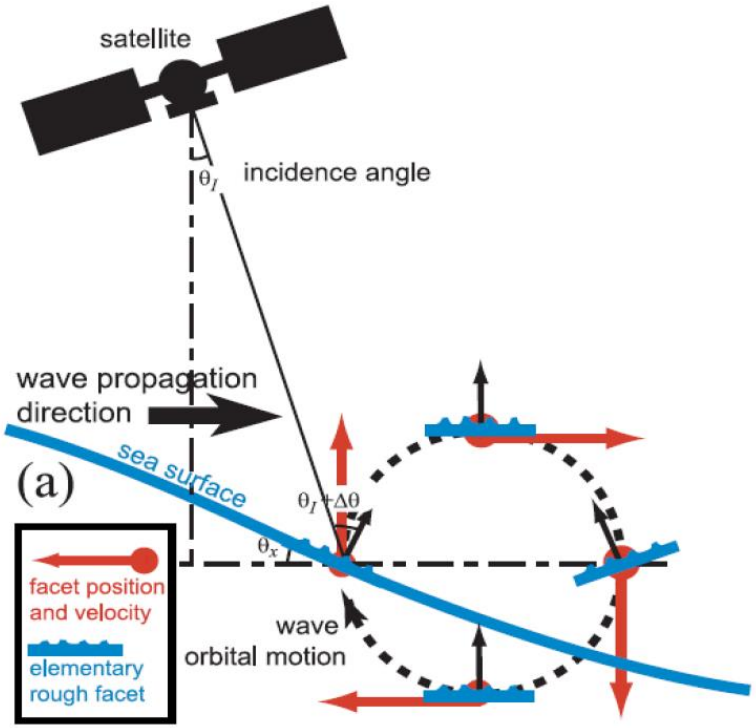

Фацетная модель :

$$\frac{\pi f_D}{k_R} = \frac{\overline{(u\sin\theta - w\cos\theta)\sigma_0(\theta+\Delta\theta)}}{\overline{\sigma_0(\theta+\Delta\theta)}}$$

$$V_D = \pi f_D / k_R \sin\theta = \bar{c} + u_S - \frac{1}{\tan\theta}\times\frac{\overline{w\sigma_0}}{\bar{\sigma}_0} + \frac{\overline{u\sigma_0}}{\bar{\sigma}_0}$$

$$V_D = u_s + \sum P_j^P(\bar{c}_j + c_j^{TH})$$

$$c_f^{TH} = \int_{k<k_L}\left[\left(-\cot\theta\times M_f^t + M_{1f}^t\right)\cos(\phi_R-\phi) + \cot\theta\times M_{2f}^h\right]\times ck^{-2}B(\mathbf{k})$$

Тип фасетов :

- Брэгговская рябь

- Гребень обрушающейся волны

- "Зеркальные" точки

$\bar{c}_j$ - скорость фасета

c_j^{TH} - добавка за счет модуляции фасетов длинными волнами

P_j^P - вклад механизма рассеяния в полную УЭПР

Background characteristics of Doppler shifts

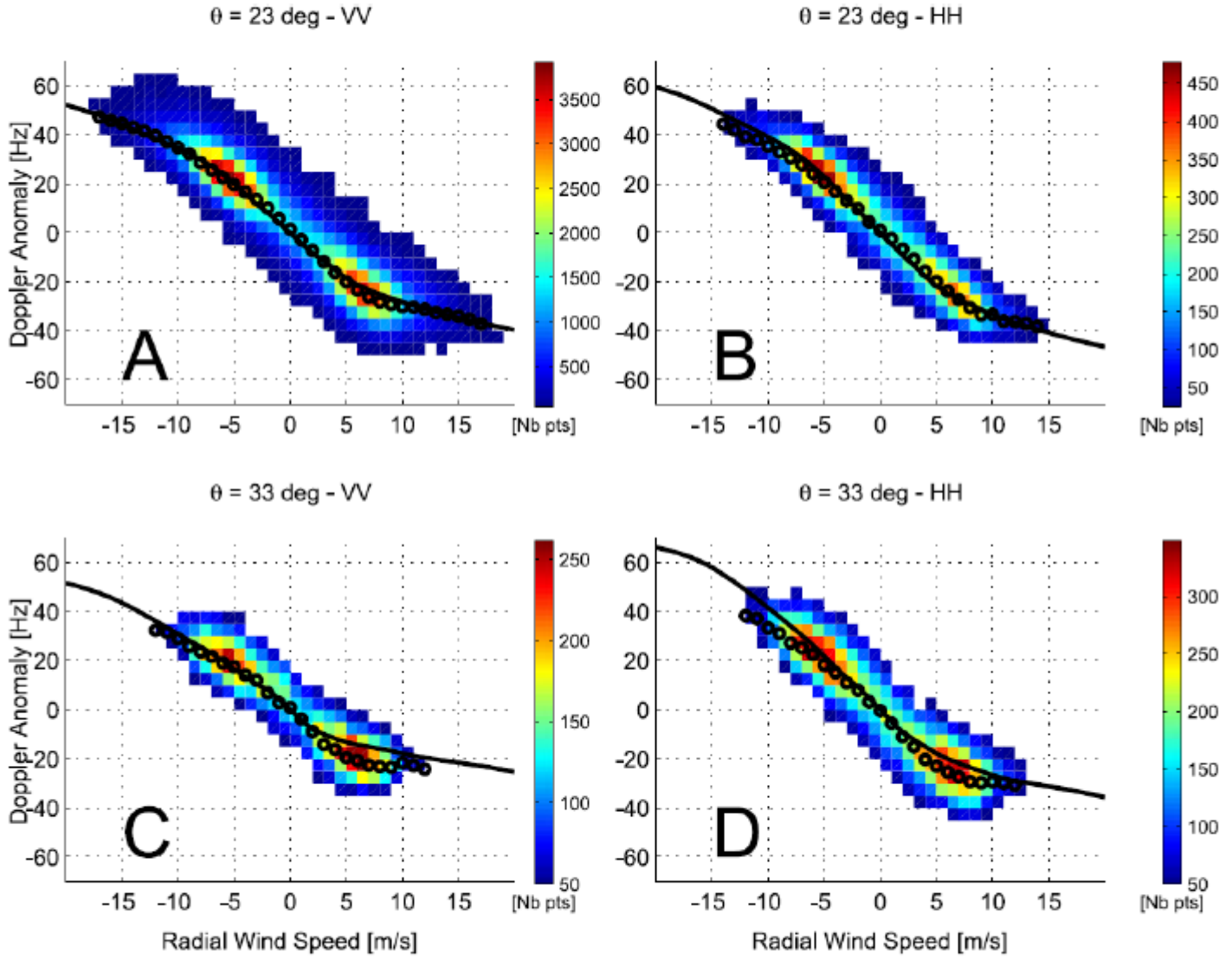

Figure 2. Observed WM (color) and simulated (solid) wind dependence of C-band Doppler shift for VV polarization in (A) and (C) and HH polarization in (B) and (D) at (top) 23° and (bottom) 33° incidence angles. The color represents the spread in number of observation points. The open circles mark the mean fit to the observations. Upwind corresponds to positive radial velocity.

- **Поля Доплеровской скорости в районе течения мыса Игольный**
- **Doppler velocities in the Agulhas current**

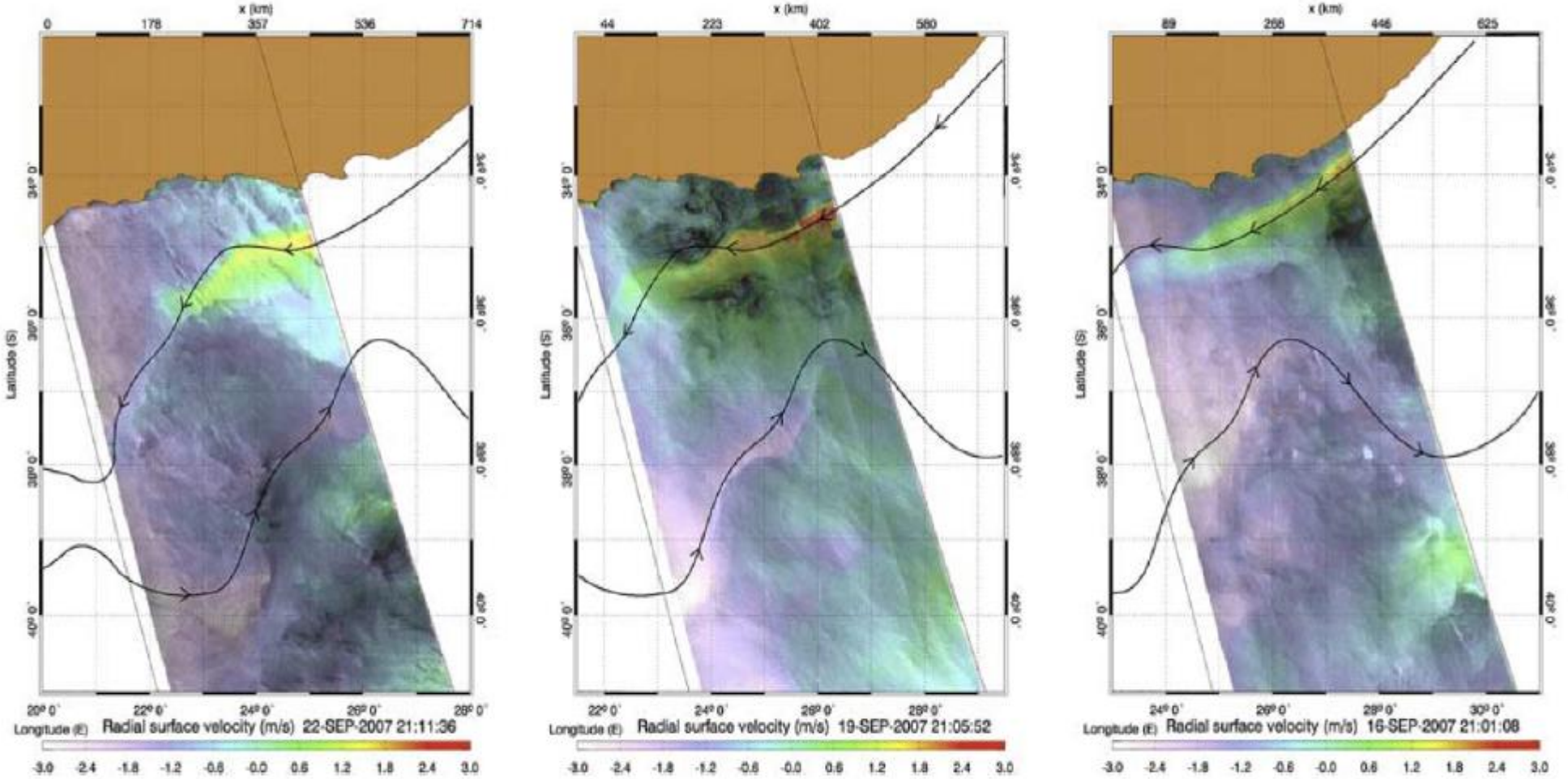

Figure 1. Time series of the Doppler velocity from the ascending ASAR wide swath (420 km) images on (right) 16, (middle) 19 and (left) 22 September 2007 covering the greater Agulhas Current region. The color bar marks the radial velocities from −3 m/s to +3 m/s. Positive speed is directed towards the SAR look direction. Black curve marks position of the maximum geostrophic current derived from altimetry 7-day mean.

Поле геострофической скорости по данным альтиметрии

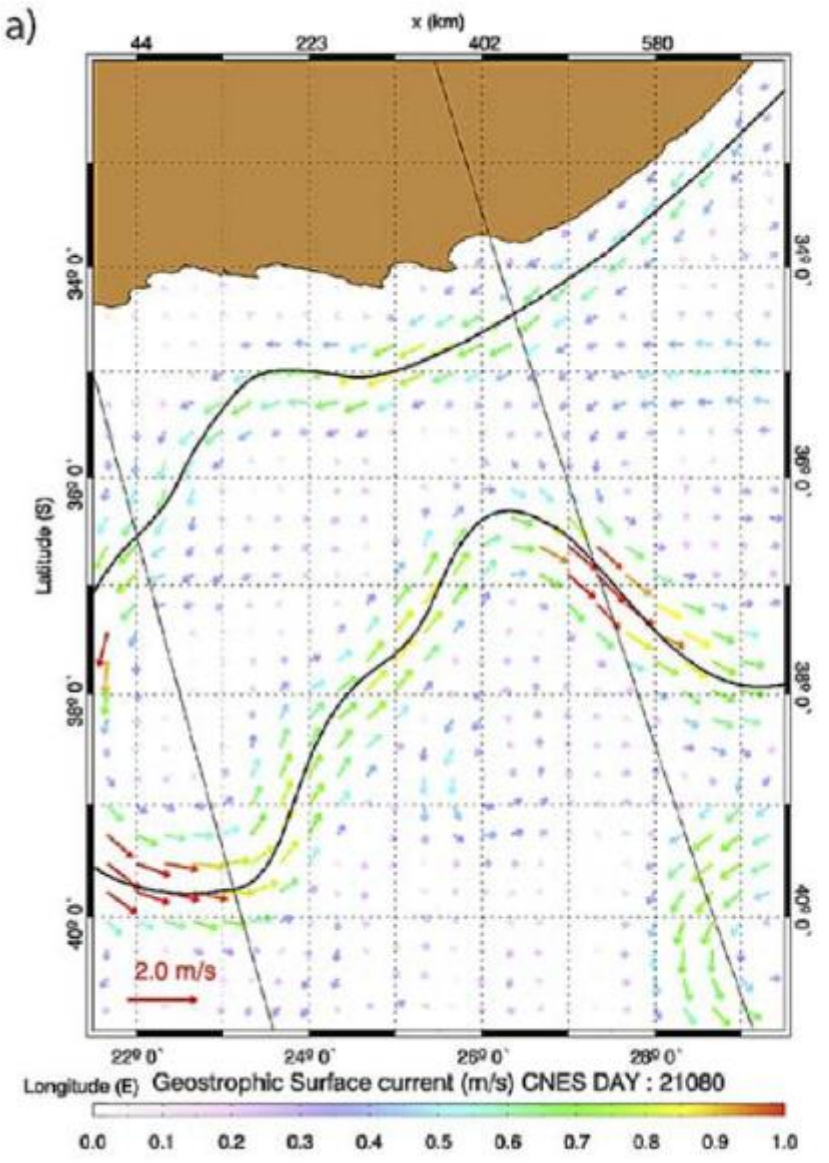

Geostrophic current from altimeter

Поле Доплеровской скорости

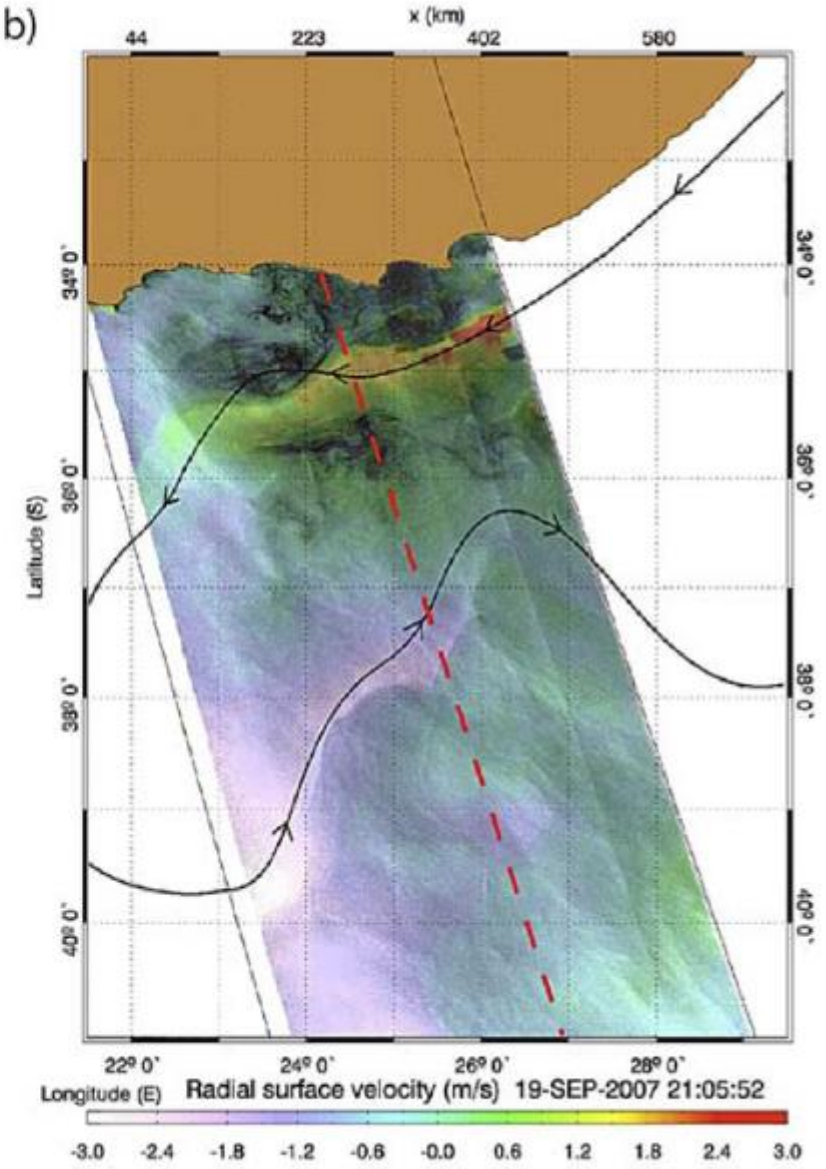

Doppler velocities

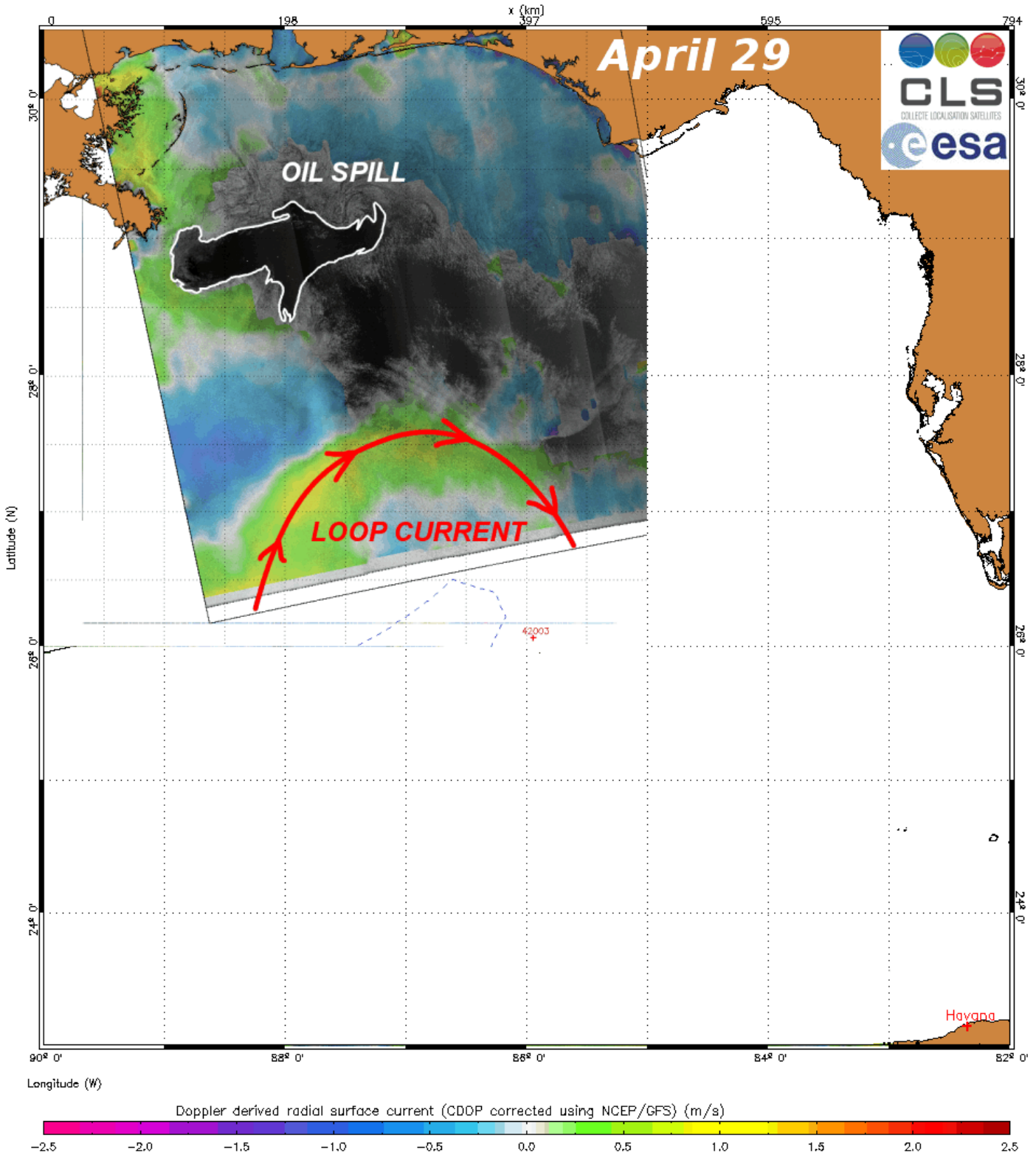
April 29
OIL SPILL
LOOP CURRENT
CLS
COLLECTE LOCALISATION SATELLITES
esa
x (km)
0
198
397
595
794
30° 0'
28° 0'
26° 0'
24° 0'
Latitude (N)
90° 0'
88° 0'
86° 0'
84° 0'
82° 0'
Longitude (W)
42003
Havana
Doppler derived radial surface current (CDOP corrected using NCEP/GFS) (m/s)
−2.5
−2.0
−1.5
−1.0
−0.5
0.0
0.5
1.0
1.5
2.0
2.5

To obtain direct ocean surface velocities from space: A speed-gun principle (Doppler analysis)

SRTM 2-Antenna Interferometry

Ultra-high resolution
Limited to line-of-sight direction

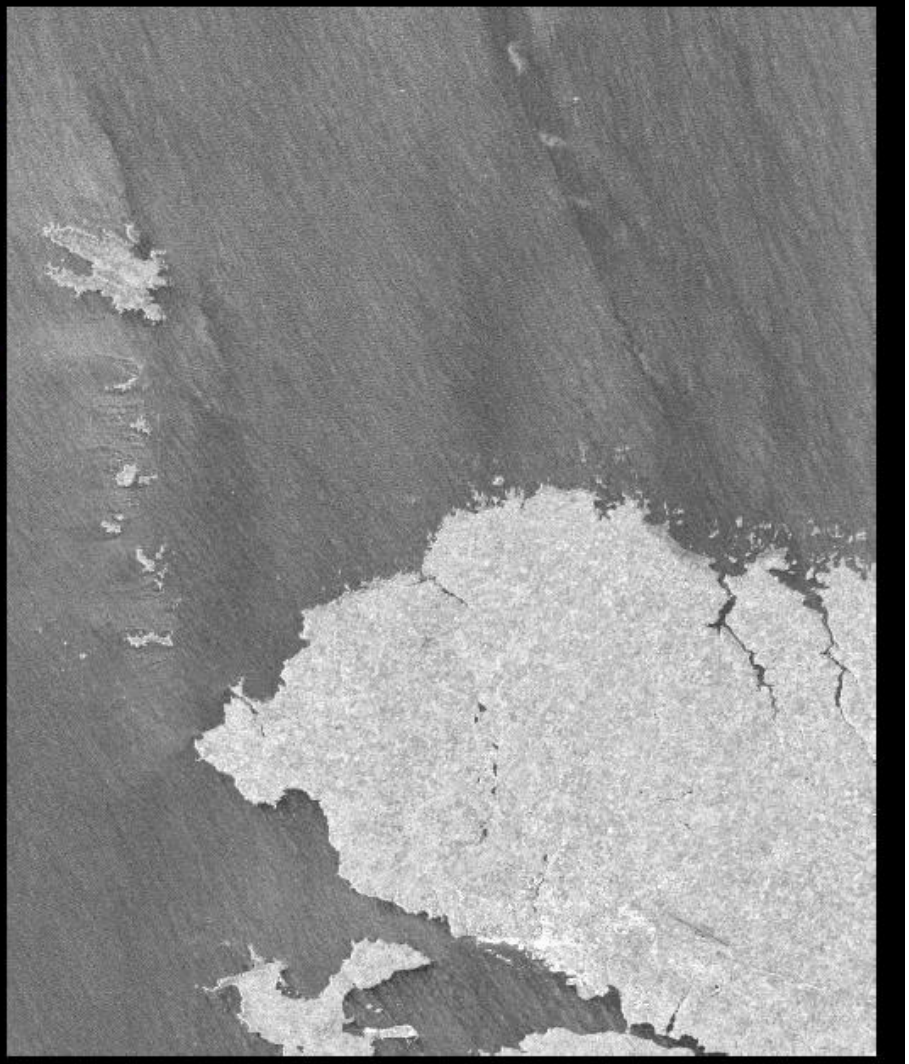

To obtain direct ocean surface velocities from space

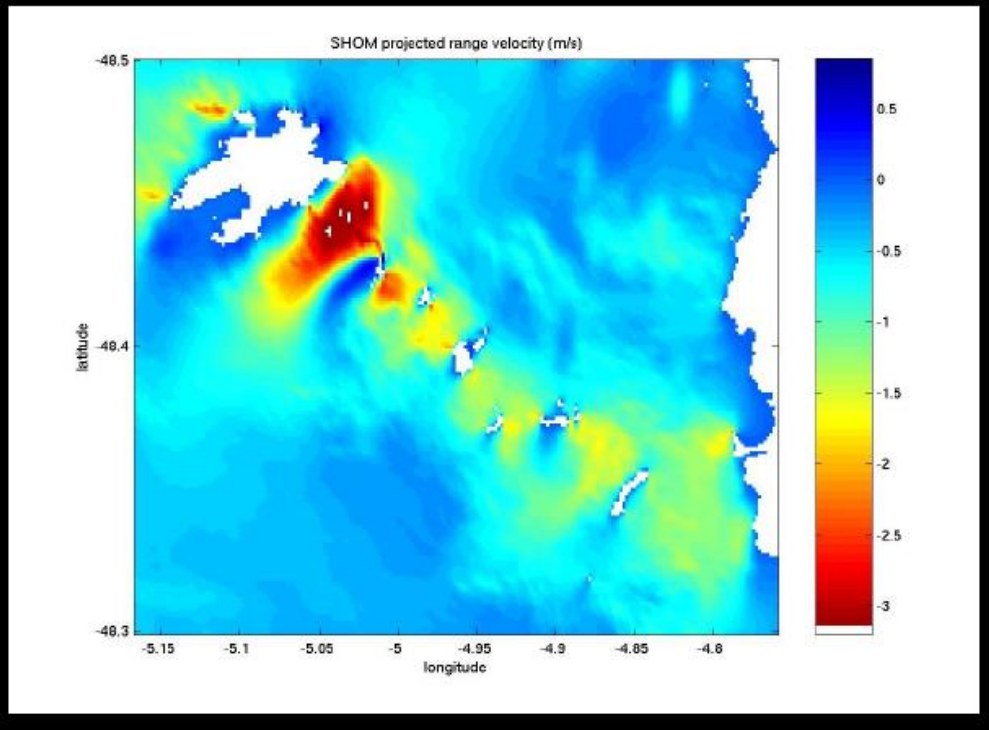

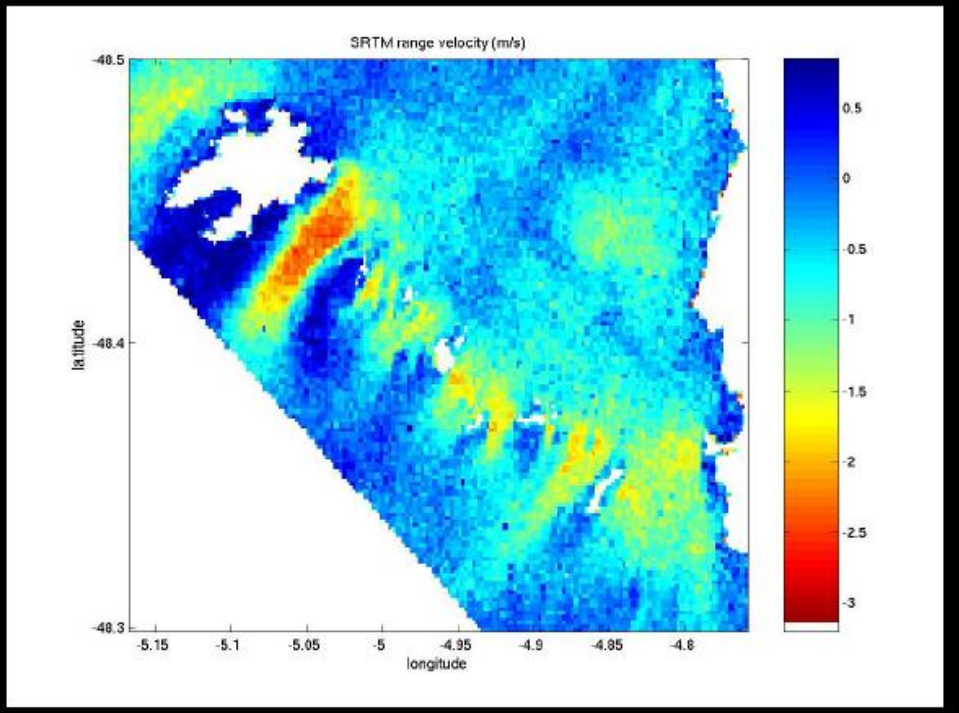

RADARSAT-1 modes (1/2)

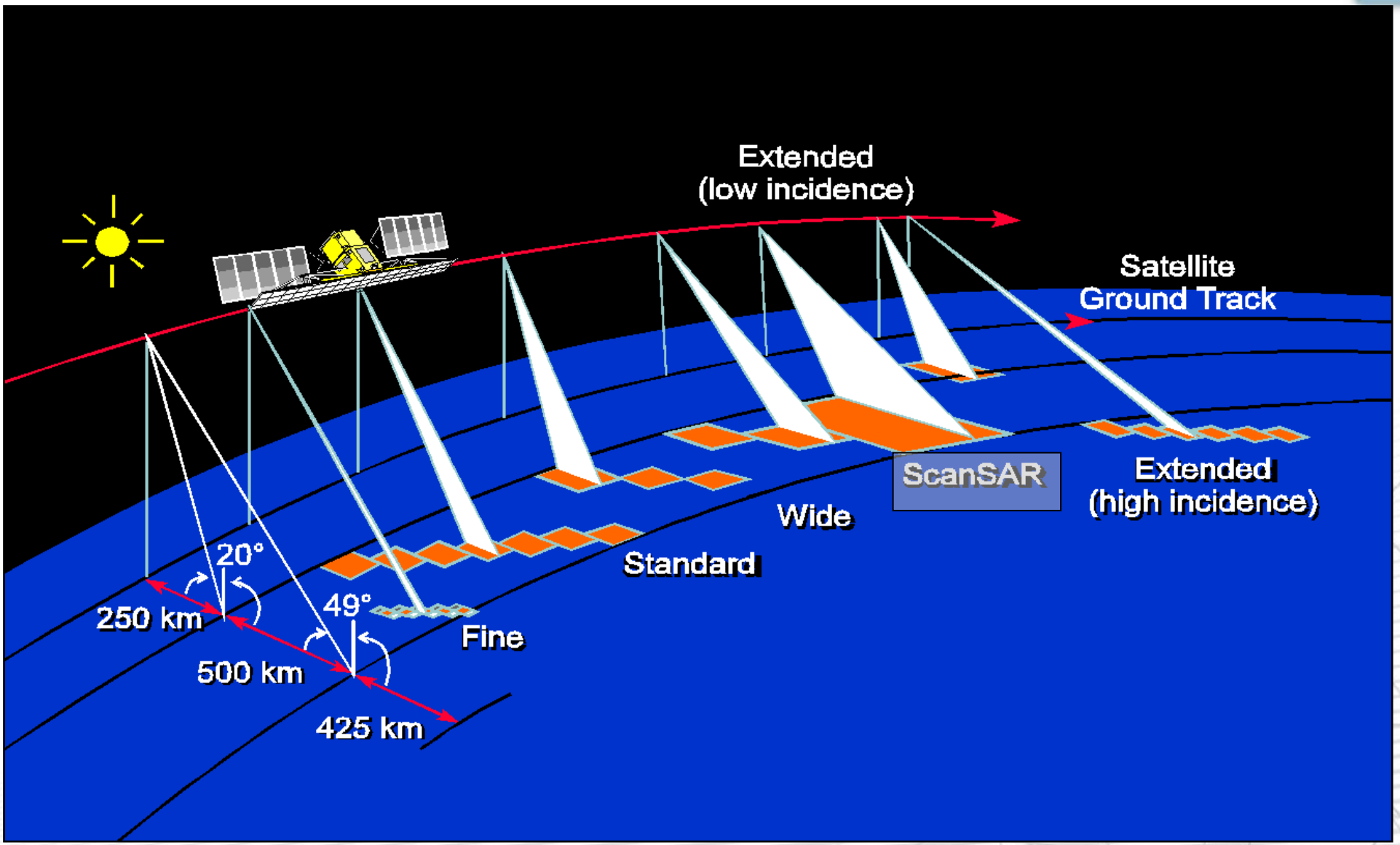

RADARSAT-1 modes (2/2)

Modes	Swath width (km)	Resolution Dist x Az (m)	Incidence angle (°)	Looks	Polarization
FINE 15 positions, 60% overlap	37 - 56	8 x 8	36 - 48	1	HH
STANDARD 7 positions, > 10% overlap	100	25 x 28	20 - 50	4	HH
WIDE 3 positions, 3% overlap	150	25 x 28	20 - 40	4	HH
SCANSAR - Narrow	**300**	**50 x 50**	**20 - 40**	**2**	**HH**
SCANSAR - Wide	**500**	**100 x 100**	**20 - 50**	**2**	**HH**
EXTENDED - High	75	25 x 28	50 - 50	4	HH
EXTENDED - Low	170	25 x 28	10 - 20	4	HH

RADARSAT-2 Features

- High resolution:
  - 3 m
  - multi-look 10 m
- Polarimetric modes
  - single/dual polarization
  - quad-pol
- Right and left-looking capability
- Enhanced ground system providing:
  - efficient satellite tasking (12 - 24 hours routine)
  - faster data processing
  - data encryption

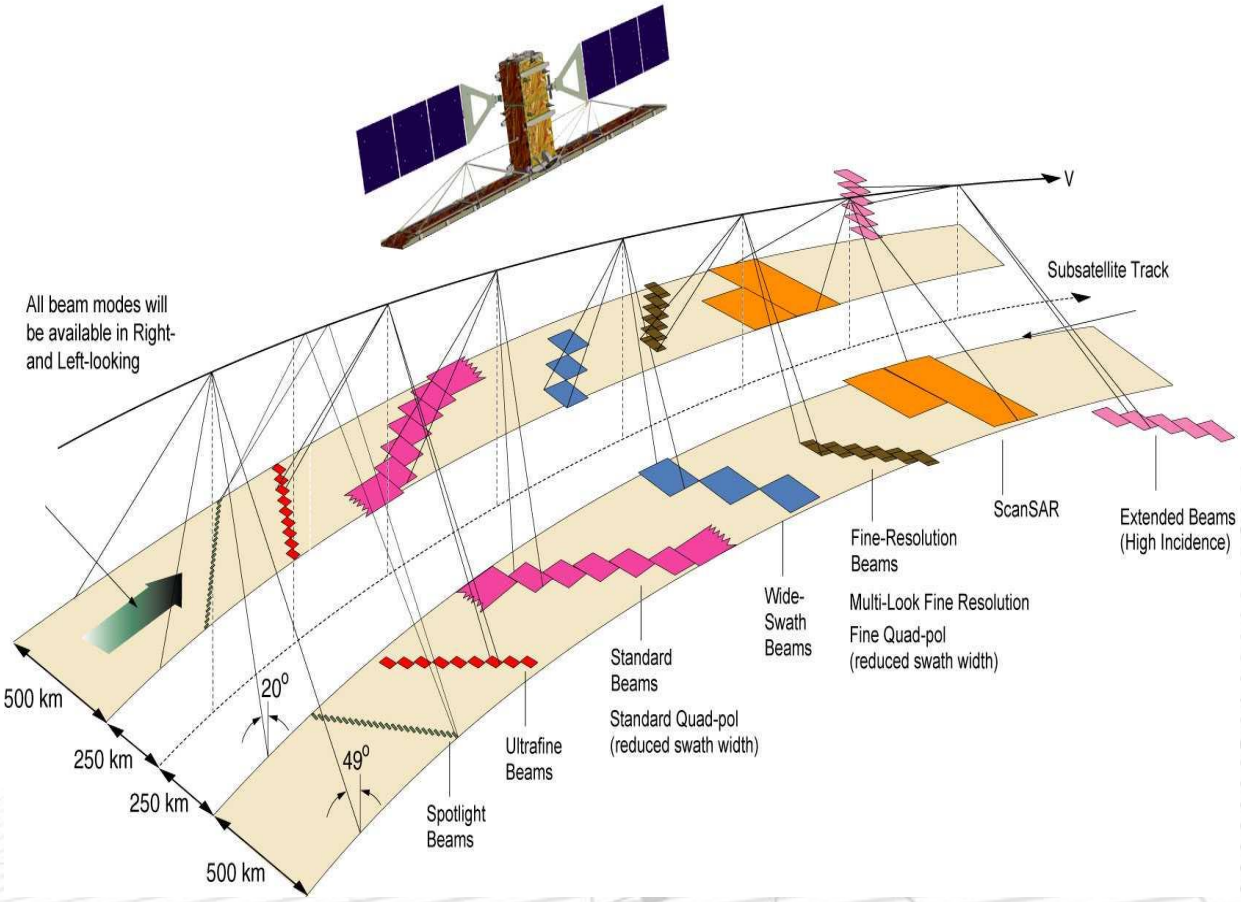

RADARSAT-2 modes

Modes	Swath width (km)	Resolution Dist x Az (m)	Incidence angle (°)	Looks	Polarization
FINE	50	10 x 9	37 - 49	1 x 1	HH, HV or VV,VH
STANDARD	100	25 x 28	20 - 49	1 x 4	HH, HV or VV,VH
WIDE	150	25 x 28	20 - 45	1 x 4	HH, HV or VV,VH
SCANSAR - Narrow	**300**	**50 x 50**	**20 - 46**	**2 x 2**	HH, HV or VV,VH
SCANSAR - Wide	**500**	**100 x 100**	**20 - 49**	**4 x 4**	HH, HV or VV,VH

Sentinel 1 (ESA)

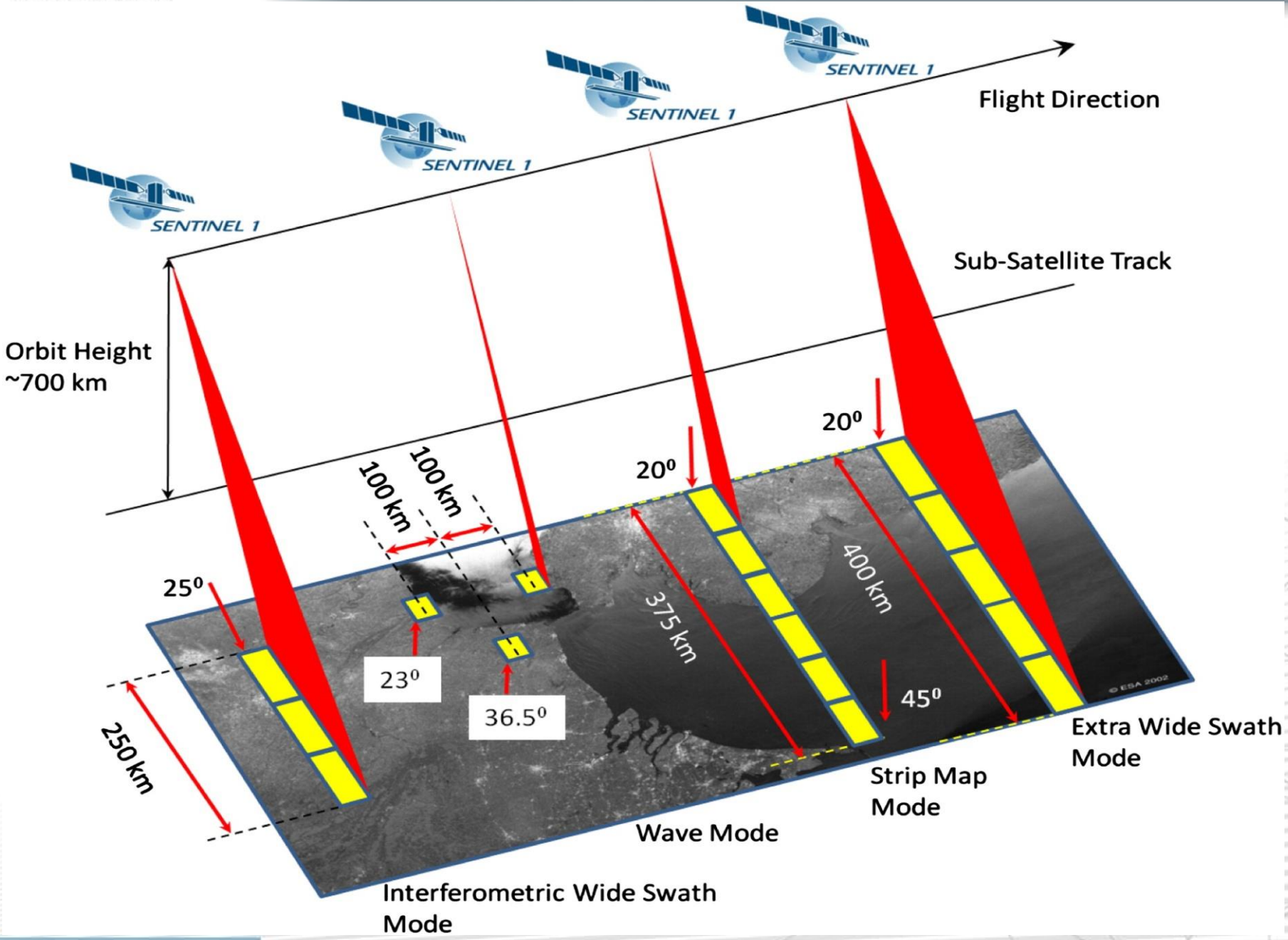

Sentinel-1 modes

Modes	Swath width (km)	Resolution Dist x Az (m)	Incidence angle (°)	Polarization
Wave (WV)	20	10 x 10	23 / 36	HH or VV
Strip Map (SM)	100	10 x 10	20 - 49	HH-HV or VV-VH
Interferometric wide swath (IWS)	250	20 x 20	30 - 45	HH-HV or VV-VH
Extra Wide Swath (EWS)	**400**	**50 x 50**	**20 - 46**	HH-HV or VV-VH